Life cycle operating energy saving from windows retrofitting in heritage buildings accounting for technical performance decay

Giovanni Litti[a,*], Amaryllis Audenaert[a], Monica Lavagna[b]

[a] EMIB Lab, Applied Engineering Laboratory for Sustainable Materials, Infrastructures and Buildings, Faculty of Applied Engineering Sciences, University of Antwerp, Campus Groenenborger – G.Z.332 Groenenborgerlaan, 171 - 2020 Antwerp, Belgium
[b] ABC Department of Architecture, Built Environment and Construction Engineering, Politecnico di Milano, Via Bonardi 9, 20133 Milano, Italy

Given the high energy saving potential obtainable from windows retrofitting, such measures are frequently implemented in the case of historic and heritage buildings. However, often, fenestration retrofitting is inter-preted as windows replacement. Rarely is the energy saving potential allowed by windows maintenance or non-destructive measures investigated. Even more rarely, the validity of retrofitting measures is assessed in the long term considering their performance obsolescence.

In this study, the Life Cycle (LC) operating energy saving potential allowed by different retrofitting options -from windows maintenance to total replacement- is discussed with regard to a heritage building in Antwerp. The study evidences that if taking into account the retrofitting interventions technical obsolescence, instead of assuming constant the technical performance throughout the retrofitting Service Life (SL), the results sig-nificantly vary. This adds a methodological concern to be considered during retrofitting design and evaluation.

The results pointed out that performing basic fenestration maintenance enables in itself Life Cycle (LC) op-erating energy savings. Moreover, it was evidenced that, destructive retrofitting techniques, such as windows replacement, not necessarily allow for the largest energy savings. Indeed the installation of single or double glazed internal windows may allow for similar or even more significant savings.

Keywords: Windows retrofitting, building, dynamic simulations, Technical performance decay, modelling Durability, Infrared thermography, Blower door test, Life cycle operating energy saving

1. Introduction

A large energy fraction in existing buildings is loss via building fenestration. According to Gustavsen et al. in [1], if considering a building with 20–30% windows surface area, the energy loss through the fenestration might be 45–60%.

For this reason, the upgrading of transparent component in existing buildings can be considered an effective option for drastically reducing their energy demand. This holds true also in case of historic buildings where, although the transparent envelope surface is limited (20% in the presented case), it is responsible for severe thermal losses via conduction and infiltration [2].

Currently, even if several fenestration improvement options are available, the one most applied also in case of historic buildings, is the total windows replacement [3]. This choice can be explained on the one hand by the large intervention affordability, technical simplicity and high energy saving potential and on the other hand by a strong lobbying activity made by window products producers and suppliers throughout the European Countries [4–6].

However, it should be noted that windows replacement is not the sole fenestration retrofitting measure allowing remarkable energy saving. Furthermore, the non-energy related drawbacks of windows replacement in historic buildings cannot be neglected. Next to the loss of building architectonic value, widely described in [3–5], a reduction of the property market value might occur [7]. Moreover, the environmental benefit of performing *anyhow* fenestration replacement in historic buildings is not always obvious from a life cycle environmental perspective because of the large initial embodied burdens [8].

For these reasons and for pursuing a more prudential approach when agreeing upon fenestration retrofitting measures in historic or heritage buildings, it is meaningful to explore the energy benefits obtainable by a wide set of retrofitting alternatives rather than confining

Received 27 December 2017; Received in revised form 9 February 2018;
Accepted 10 February 2018
Available online 17 February 2018

* Corresponding author.
E-mail address: giovanni.litti@uantwerpen.be (G. Litti).

Abbreviations: ERI, energy retrofitting interventions; *EERI*, energy environmental retrofitting interventions; *EPBD*, energy performance building directives; *SL*, service life; *EOL*, end of life; *EOSL*, end of service life; *RSL*, reference service life; *BDT*, blower door test; *ACH*, air change per hour; *IRT*, infrared thermography; X_1, X_2, physical properties with regard to building assemblies or components initial (1) and deteriorated (2) state of conservation; *Nu*, Nusselt number (-); λ, thermal conductivity (W/m K); *R*, thermal resistance (m^2 K/W); *U*, thermal transmittance (W/m^2 K); η_{50}, air infiltration rate at 50 Pa (h^{-1}); η_{nat}, standardized air Infiltration rate (h^{-1})

Published Journal Article available at: https://doi.org/10.1016/j.jobe.2018.02.006

Table 1.1
Description of fenestration improvement scenarios discussed in the study.

Scenarios	Activities
1. Baseline model	No activities foreseen
2. Fenestration maintenance and restoration	Re-putty of glass bars, frame painting and window restoration
3. Fenestration drought proofing	Sealing of window sashes and fixed frame edges + scenario 2
4. Indoor storm-glazing addition	Addition of internal secondary glazing + scenario 2 + scenario 3
4.1. (α) Indoor storm-glazing addition	Addition of internal secondary glazing (single glazing) + scenario 2 + scenario 3
4.2. (γ) Indoor storm-glazing addition	Addition of internal secondary glazing (IGU) + scenario 2 + scenario 3
5. Glass panes replacement	Replacement of the existing window glass panes (IGU) + scenario 2 + scenario 3
6. Fenestration replacement	Replacement of the entire window unit
6.1. (A) Fenestration replacement	Replacement of the entire window unit (Aluminium frame)
6.2. (PVC) Fenestration replacement	Replacement of the entire window unit (PVC frame)
6.3. (T) Fenestration replacement	Replacement of the entire window unit (Timber frame)

the decision making to the apparently most performing option.

The first objective of this study is to compare life cycle operating energy saving allowable by eight fenestration-retrofitting scenarios and sub-scenarios ranging from non-invasive to destructive interventions; see Table 1.1. The retrofitting alternatives are modelled for the Schoonselhof Kasteel, a public monumental building in Antwerp.

Because materials and components within a building assembly deteriorate, any retrofitting intervention undergoes technical decay over time. We believe that this aspect should be taken into account within the Energy and Environmental Retrofitting Interventions (EERI) modelling and decision-making as it may strongly affect the results and even invalidate the taken decisions if based on the assumption that EERI keep constant technical performance until the assemblies End Of Service Life (EOSL). In the literature this concern is marginally explored [9–11], and only addressed in theoretical or probabilistic terms and not from a building physic point of view integrating dynamic building simulations with materials deterioration modelling.

The second objective of the study is to quantify the operating energy saving fraction lost due to the technical performance decay of each (windows) perishable component and to integrate it within the quantification of the life cycle operating energy of each modelled sub-scenario. Variations of intervention iteration frequency and materials Service Life (SL) were also considered resulting in a total of 120 modelled sub-scenarios.

The relationship between materials durability and life cycle operating energy is discussed in Section 2. The windows perishable components considered in this study and their technical deterioration are discussed on basis of a dedicated Literature review in Note 1 in Supplementary material.

In order to achieve the mentioned objectives, it were undertaken the research tasks plotted in Fig. 1.1 and below discussed.

From onsite assessment (Sections 3.1 and 3.2) input data for the simulations were acquired, more specifically for modelling: baseline, maintained and drought-proofing -scenarios (scenarios from 1 to 3 in Table 1.1). Moreover using the onsite performed tests, it was possible to determine the initial and deteriorated performance of some materials considered in the retrofitting scenarios.

Based on the acquired data, a steady-state windows model was performed and calibrated (Sections 3.3 and 3.3.1). The calibrated windows model was used for obtaining input data for running the dynamic building simulations of scenarios from 1 to 5. The dynamic simulations were run twice: firstly considering the windows perishable components in their initial state (obtaining the scenario energy consumption in its initial state) and secondly in their deteriorated state (obtaining the scenario energy consumption in its deteriorated state). General modelling assumptions and methodology are discussed in Sections 3.3 and 3.3.2, while specific considerations on the initial and deteriorated scenarios modelling are described -per scenario- in Section 3.5.

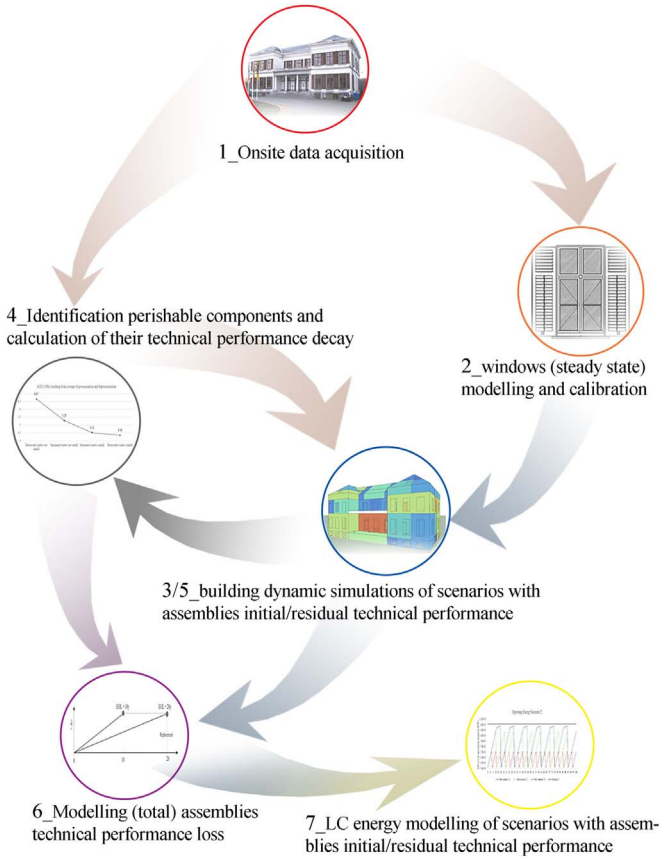

Fig. 1.1. Research flow chart; the arrows and numeration display respectively the activities interrelation and sequence.

The deterioration causes of the considered (windows) perishable components were identified from literature research (see Section 2 and Note 1 in Supplementary material). The effect of this deterioration on the alteration of the windows technical performance was modelled according to onsite measurement, literature results and existing standards. A new modelling proposal (see Section 3.4). Modelled retrofitting scenarios are described in Section 3.5, study results are discussed in Section 4 and conclusions in Section 5.

Note that this study does not focus on the whole Life Cycle Assessment of the presented EERI, hence, initial and recurrent embodied energy is not accounted; only building operating energy for space heating is considered. The considered building Reference Service Life (RSL) is 100 years.

1.1. Energy retrofitting interventions in historic buildings: a framework

The need to reduce existing buildings energy demand by means of Energy Retrofitting Interventions (ERI) as solicited by the 91 and 31 European Building Directives (EPBD) [12,13] is an ethical commitment before being a political challenge. The implementation of EERI not only can allow substantial green gases emissions reduction, but it can also enable sustainable economic growth and job creation [14]. From this process also the Historic Built Environment is meant not to be excluded. A study from BPIE concluded that minor or moderate retrofitting interventions can likely be applied in historic and heritage buildings[1] allowing energy demand reduction by up to 60% [15,16].

However, given the lack of a dedicated European legislative framework, aimed at bridging the gap between EPBD and Conventions for historic and heritage buildings protection, there may be a risk of speculation justified by the need of making the historic built environment more energy efficient. The cultural and economic price paid until now because of the ongoing speculation is unknown. It is unknown not because there has not yet been damage to the historic buildings but rather because we still lack appropriate metrics for precisely quantifying the cultural and economic consequences of this loss of value.

According to a study from English Housing Survey [7], 52% of historic houses built in the UK before 1919 now have new PVC window systems. It is hard to believe that this massive fenestration replacement is the result of design praxis undertaken "with great sensitivity to the preservation of the unique quality of the individual building" as suggested in [14] or without "alteration to the character or appearance of the buildings" as stated in article 4 of both the EPB and EE Directives [12,13,17]. In these cases, although the building energy demand was consistently reduced, valuable art crafts have been definitely lost compromising the buildings architectonic significance as well as their market value. Moreover, it is not clear whether these interventions were legitimated by life cycle benefits not similarly obtainable by alternative non-destructive retrofitting options.

A survey made by English Heritage in 2009 and cited in [7], showed, that the replacement of doors and windows in conservation areas have constituted the biggest threat to the properties economic values. 82% of interviewed estate agents confirmed that historic features add financial value to historic properties, conversely, recent building alterations or spontaneous superfetations might reduce it [18].

An example of windows replacement in a historic non- protected building that, in the authors opinion, is likely to alter its market value is given Fig. 1.1.1. At the ground floor of an early XX Century building in Antwerp, a finely carved timber window was retained on the left ground floor apartment, while it was substituted by an aluminium window on the right one.

The discussion so far, does not mean that energy efficiency improvements of historic buildings should be forbidden, rather it means that a tout court implementation of destructive solutions when dealing with this kind of buildings might be an inappropriate approach for the following reasons:

1) We do not have sufficient metrics for a complete assessment of the long-term EERI consequences;
2) The widely accepted hypothesis according to which, any building economic value reduction caused by the destruction of architectonic features (such as historic windows) will be compensated by the increased building economic value allowed by the increased energy performance, needs to be seriously reconsidered.
3) Several of the currently implemented EERI resort to technologies that enable energy savings achievable by other –less invasive- techniques.

[1] The BPIE considers historic and heritage buildings the ones built before 1900; see annex 2, point b; in [16].

1.2. Fenestration retrofitting in historic buildings: environmental and architectonic implications

The evaluation of the environmental and architectonic impacts given by the implementation of energy saving measures in historic buildings fenestration is not a recent matter. In 1996 the Swedish Directorate for Cultural Heritage commissioned the Norwegian Building Research Institute to undertake a study for evidencing the life cycle environmental impacts of different windows retrofitting options in historic buildings [8]. The study, in contrast with the 93/76/EEC Standard, concluded that the replacement of historic windows does not allow energy saving substantially higher than the ones allowed by other techniques such as the addition of an inner glazing pane. Hence, windows replacement was discouraged because of the high initial embodied impacts. Similar conclusions were reported in the same year in a study commissioned by the Historic preservation Division of the State of Vermont (USA) to the University of Vermont [19].

Notwithstanding that information about alternative options to windows replacement was available already at the end of the '90 s, several Countries (in agreement with the 93/76/EEC Directive) continued distributing governmental subsidies for boosting historic windows replacement instead of promoting fenestration repair or improvement. Rare were the cases, such as the one of Federal Commission for the protection of historic monuments in Switzerland, in which Governmental institutions, allowed public subsidies only in case of non-invasive historic fenestration retrofitting [20].

In 2006 the 93/76/EEC (SAVE) Directive was repealed, but during the 13 years of its implementation, an uncountable loss of historic windows in Hungary, Finland, Norway and UK was registered [4,21].

2. Relationship between materials performance decay and building life cycle operating energy

Materials undergo aging and decay over time; likewise for materials or components making up a building assembly. This deterioration may result in a technical performance reduction for the entire assembly (e.g. windows), and in turn for the whole building.

Generally building assemblies lose their initial performance over time, therefore their contribution to energy saving is not constant until their replacement [11,22]. In fact, physical, chemical, or biological deterioration of components within an assembly may alter their materials density or thermal conductivity (technical decay). This results in an overall assembly mechanical, thermal or other technical performance decay [23–27].

Components technical obsolescence not only can alter the initial assembly performance, but it can even bring forward its technical End Of Service Life (EOSL) by reaching a performance level (e.g. thermal transmittance) lower than the one that had justified its initial installation. Because of this, most of the authors focus on the estimation of assemblies EOSL. This estimation is traditionally performed by means of factorial-based, probabilistic (stochastic) or engineering models [11,22,28,29]. However, because of the high uncertainty of the involved variables in the process of materials aging, it is difficult to perform an accurate forecast of the assemblies EOSL.

In the authors opinion, the mentioned issues should be addressed not only in terms of assembly EOL prediction, but by quantifying the life cycle operating energy alteration consequent of materials decay. In other words, accounting for the assemblies durability as defined by Daniotti in [22]. This is because, materials decay not only reduces assemblies SL, but also their technical performance; this is true especially in the case of historic buildings. Indeed, in this kind of buildings, the state of conservation of traditional materials themselves may trigger anticipated deterioration of retrofitting assemblies compromising their expected performance or even anticipating their failure [30].

Though it is widely documented that technical decay of retrofitting assemblies prevents constant energy saving over time [31–33] and

Fig. 1.1.1. Windows replacement in a not protected historic building, Antwerp (Litti).

recent studies solicit its integration within the EERI modelling and evaluation [9,34], this issue is insufficiently discussed in the literature. Only a few contributions introduce this concern [10,35,36]. Nevertheless, in those contributions the technical performance decay was either modelled by means of probabilistic scenarios or by accounting the effect of only one components deterioration on the steady state building energy use. The effect of the physical deterioration of each perishable components of the implemented retrofitting on the building life cycle operating energy -by also taking into account different replacement frequencies and materials SL- has not yet been addressed.

Note 1 in Supplementary material gives the theoretical background of the technical deterioration for the perishable components considered in this study and related references.

3. Research methodology and scenario description

In this section, the research methodology with regard to onsite measurement activities, steady state windows simulations, dynamic building simulations and technical decay modelling are discussed. Moreover, each scenario is individually described considering the theoretical assumptions and limitations.

3.1. Case study description

The case study discussed in this contribution is the Schooselhof Kasteel in Wilrijk, Antwerp (Belgium). The building was constructed in its current outlook between 1830 and 1840 in neoclassical style (see Fig. 3.1.1). The property, owned by the Municipality, will be renovated in the coming years for hosting new functions other than offices as in its present state. Although the building houses administrative offices, only a few rooms of the building are currently in use.

The building is equipped with heating system (gas condensing boiler, 180 kW) in two floors on four: ground and first floor (total heated area $\approx 700\,m^2$). Because insulation between heated and unheated spaces is missing and building envelope shows severe conservation issues especially on the windows, ad hoc retrofitting measure are urged for improving both energy efficiency and indoor microclimate quality [37].

Fig. 3.1.1. Schoonselhof Kasteel, South façade.

The existing windows were installed between 1830 and 1840. In 1921 a first maintenance intervention aimed at their restoration and varnishing occurred [39]. Later, in 1947, a second extensive intervention was performed as the windows were damaged by the WWII bombing. During this intervention, windows frames were restored and broken glass panes replaced. The last documented restoration during which windows maintenance occurred is in 1956. Successively, no specific interventions on the fenestration were reported. In the last ten years, sporadic works on the windows were undertaken mainly aimed at installing provisional timber reinforcements after episodes of burglary and sealing with silicone the gaps between glass panes and frame bars of the few in-use building rooms at the ground and first floor.

The existing fenestration, including joinery, ferruling and opening systems, might be considered an example of the Belgian windows manufacture up to 1880 [40]. The window typologies for the four building storeys are shown in Fig. 1 in Supplementary material, while their poor state of conservation due to lack of putty on windows glazing bars, water absorption (because of paint layer decay) and rotting of timber is shown in Figs. 2 and 3a and b in Supplementary material.

As mentioned, the general state of conservation of the building fenestration is poor. Nevertheless, in few rooms, because of their continuous use, basic windows maintenance has been performed. The maintenance consisted in filling with silicone the glass bars (re-putty). In all the other rooms, the application of the putty occurred about 10 years ago; in these rooms, the putty is completely absent or severely damaged (Fig. 2 in Supplementary material).

3.2. Onsite building assessment: blower door test (BDT) and infrared thermography (IRT)

In order to acquire input data for running the simulations and quantifying the building energy consumption consequent to different windows state of conservation, a Blower Door Test (BDT) was performed in two rooms in which maintained and non maintained windows, respectively putty recently applied and putty applied over 10 years ago, are present.

From now on, the two spaces are named respectively space 1 (non-maintained) and space 2 (maintained). The two rooms have identical state of conservation of opaque envelope and identical orientation (North-West). The net room volume for space 1 and 2 is respectively is $\approx 80\,m^3$ and $\approx 160\,m^3$. The windows surface of the two monitored spaces, represents 11% of the total net fenestration area of the heated part of the building.

The BDT in the two spaces was performed according to method B in EN 13829 [41]. Each space was prepared for the test by taping with air impermeable tape the potential grey infiltrations beyond the scope of the measurements. The infiltration/exfiltration air change rate through the façade and fenestration was quantified respectively in depressurization and pressurization test modality.

In space 1 at the ground floor, the average air change rate from pressurization and depressurization at 50 Pa (η_{50}), was 6.67 (h^{-1}), while

in space 2 at the first floor it was 5.39 (h^{-1}). For obtaining the natural air change rate (η_{nat}), the two values, were standardized as reported by Dickerhoff in [42] and Sherman in [43], namely dividing them by 20. The authors obtained the mentioned relation by regressing the air leakage against the air infiltration of a large sample of buildings.

The obtained natural air change rates were considered for the simulations of scenario 1 and 2 in turn (Table 1.1).

During the test, Infrared Thermography (IRT) was performed in order to localize air leakages through the window elements for later deciding upon the positioning of the sealant.

In Figs. 4a and b and 5a and b in Supplementary material the air infiltrations at the sashes meeting and through sashes, sills and jambs are visible. In Fig. 6a and b in Supplementary material, it is possible to observe the infiltrations through the glass bars on the window sashes.

Beside the localization of air infiltrations, IRT was performed for allowing the calibration of the model of the existing windows, see Section 3.3. For this purpose, the windows frame and glass surface temperature were measured with thermal imaging after the measurement of current frame emissivity. For minimizing the influence of solar radiation, the measured windows had closed shutters as of the previous day. The frame emissivity was measured by using a black tape (emissivity 0.97) and taking into account the actual environmental conditions.

In order to exclude from the frame heat transfer the infiltrative contribution, also neglected in the steady-state windows model, the IRT was repeated when the window units were sealed. Indeed, to acquire data for running the simulations aimed at quantifying the potential improvement allowed by windows draught proofing, the windows from both the spaces were sealed with air impermeable tape emulating a draught-proofing intervention (scenario 3 in Table 1.1). The precise positioning of the tape onto the windows is given in Fig. 3.5.3.1. IRT and blower door test were, hence, repeated for controlling the goodness of the performed window sealing. After the drought-proofing, the infiltration rate at 50 Pa (η_{50}) in space 1 and 2 was 4.36 (h^{-1}) and 4.52 (h^{-1}) respectively.

From Figs. 7a and b and 8a and b in Supplementary material is possible to observe the correction of the air infiltration on the central and angular part during depressurization test of draught proofed windows in space 1. It can be seen that only radiative and conductive losses are present but not infiltrative ones. The BDT results are plotted in Fig. 3.2.1.

By looking at Fig. 3.2.1, it can be observed that windows maintenance, namely the re-putty of glass bars, allowed to decrease infiltration rate by up to 21% compared with non-maintained windows (comparison space 2 VS space 1). The addition of drought-proofing reduced infiltration rate of extra 16% (comparison mean drought proofed VS space 2). In other words, the sealing of the window sashes and edges allowed to reduce infiltration rates by up to 37% compared to non-maintained windows. Similar results were found by Basset and D'Ambrosio in [44,45].

It is worth considering that when the historic windows, in both the spaces, were completely sealed, the air change per hour was almost identical: variation smaller than 4%. This confirms the findings from James et al. in [19]. The identical air infiltration rate in both the spaces, stands for the maximum air tightening improvement achievable by intervening on the windows tightness. The mean of the two values was considered in the study and standardized as mentioned above. It should be clarified that the obtained air change per hour after the windows sealing is not only the lowest one achievable if sealing the existing historic windows, but it is the lowest one achievable by any window installed in the measured spaces. For this reason, the obtained standardized mean value is used as input data in all the models from scenario 3–6, see Table 1.1.

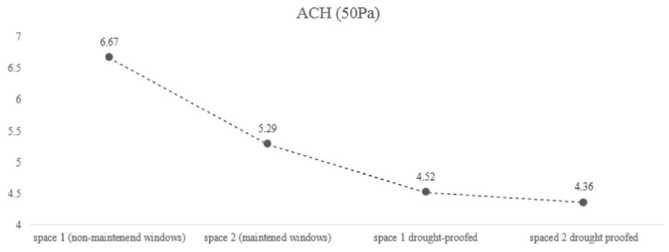

Fig. 3.2.1. Air change per hour of maintained (space 2) and non-maintained (space 1) windows before and after the draught proofing; on the y axis are reported the ACH values at 50 Pa.

3.3. Case study simulations

Before running dynamic simulations at building scale, a preparatory study in steady state regime (solely targeted at the windows) was performed. The study, performed with the software THERM and WINDOW (versions 7.4) aimed at modelling and calibrating the existing windows. The physical parameters after the windows model calibration were inputted in the building dynamic simulations.

THERM, developed by the Lawrence Berkeley National Laboratory (LBNL), is a simulation software used for the two-dimensional heat-transfer modelling of building components. The software was integrated with the WINDOW software glazing library. More details on THERM and the finite elements heat transfer calculation methodology implemented in the software can be found in [46].

Successively, the building dynamic simulations were performed with the software VE (Virtual Environment) developed by IES (Integrated Environmental Solutions). More on the transient calculation methodology implemented in the software package can be found in [47].

3.3.1. Windows simulations

In this preparatory study, one window at the ground floor (space 1) was selected for the calibration. The surface temperature distribution of the modelled window in THERM was compared to the one measured onsite with IRT imaging. In-situ measured environmental boundary conditions and materials emissivity were inputted in the window model; hence, the thermal conductivity from the modelled window frame was tuned for minimizing the deviations.

The boundary conditions at the indoor/outdoor air/surface interface were modelled using constant heat transfer coefficients calculated with the air temperature in-situ measured (outdoor 11 °C, indoor 20 °C) according to Annex A in [48]. The surface resistance of the adjacent surfaces inputted in the simulations were calculated according to annex A in [48], see Eq. (1) below.

$$R_{si} = \frac{1}{h_c + h_r} \tag{1}$$

where h_r is the radiative coefficient and h_c is the convective coefficient calculated according to Annex A in [48]. The surface emissivity for the painted window frame is 0.90. The outdoor and indoor radiative coefficient is respectively 4.59 and 5.13 W/m^2 K. The indoor convective coefficient is considered 2.5 and 5 W/m^2 K respectively for horizontal and upwards heat flow while the outdoor one is 16 W/m^2 K (wind speed 3 m/s during the measurements). Therefore, the indoor and outdoor resistances inputted in the model are respectively 0.13 and 0.05 m^{2}K/W for the vertical windows, while for the skylights (at the attic level), they are 0.10 and 0.05 m^{2}K/W.

The thermal conductivity of the timber frame in THERM was adjusted by considering ± 0.1 W/m K step intervals starting from 0.20 W/mK. All the control points showed closer surface temperature values with thermal conductivity 0.23 W/m K, see Table 3.3.1. It is worth mentioning that most of the wood qualities reported in Table 3.39 in CIBSE, Guide A [49] have thermal conductivity ≈ 0.23 W/m K when moist.

Table 3.3.1
Measured and simulated windows; surface temperature comparison.

Control point localization	Description	Image	Measured (FLIR E60bx IR Camera) Min temp (°C)	Max temp (°C)	Instrumental average (°C)	Simulated (THERM 7.4) Min temp (°C)	Max temp (°C)	Average (°C)	Deviation from the mean (°C)
upper frame	central part of the operable frame	3.3.2	17.7	18.5	18.4	17.10	18.00	17.55	0.85
upper sill	central part of the sill	3.3.2	18.8	19.3	19.2	18.40	19.30	18.85	0.35
Upper connection point	towards connection with the sill	3.3.2			17.9			17.00	0.90
lower frame	gap connection fixed/ operable frame	3.3.1	15.7	17.5	16.7	16.30	17.50	16.90	−0.20
lower sill	central part of the sill	3.3.1	17.6	18	17.8	17.70	19.20	18.45	−0.65
glass pane		3.3.1			15.6			17.10	−1.50
glass bar	central part of the bar	3.3.3	18.4	18.6	18.5	18.30	18.60	18.45	0.05
transom	central part of the operable frame	3.3.3	18.5	18.6	18.6	17.10	18.10	17.60	1.00
Transom upper point	upper part of the fixed frame	3.3.3			18.7			18.00	0.70
			Instrumental accuracy 2% of measured value						

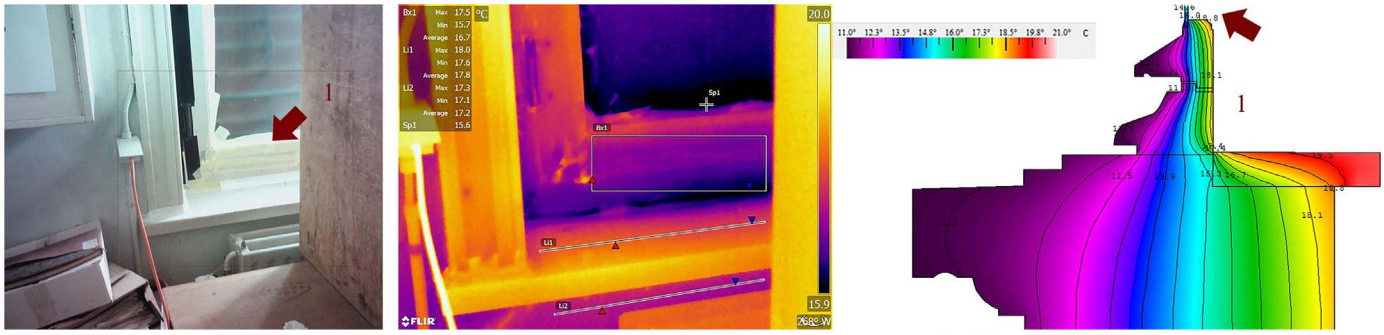

Fig. 3.3.1. (a)–(c) Inferior window frame connection; from the left (a) corner localization, (b) IRT imaging, (c) window model (THERM 7.4).

The results from the steady state windows model calibration are summarized in Table 3.3.1 and presented in Figs. 3.3.1(a)–(c), 3.3.2(a)–(c) and 3.3.3(a)–(c).

Although the model tends to overestimate the surface temperature of the lower part of the window frame and to underestimate the one of the upper part, the observed absolute deviations are only in one control point higher than 1 °C.

In Fig. 3.3.1(a)–(c) the inferior frame profile is shown. The control points show that the model simulates frame surface and sill temperature slightly higher than the one infield measured. Similar is the case for the surface temperature of the glass pane. In the latter case the temperature deviation is 1.5 ± 0.31 °C, the highest deviation registered in the model.

In Fig. 3.3.2(a)–(c), the superior frame profile is shown. In this upper part, differently from the lower one, the model tends to underestimate the surface temperature of the frame. For the upper control points, the maximum deviation between measured and simulated surface temperature is 0.9 °C.

In Fig. 3.3.3(a)–(c), two different parts on the central/upper part of the window frame are shown (horizontal glass bars and transom). Also in this case the model tends to underestimate the surface temperature. However, the maximum deviation between measured and simulated values is lower than 1 °C.

The reasons for the obtained discrepancies between simulated versus measured windows frame surface temperature, may be explained as follows. In the model, a steady indoor air temperature 20 °C was set as indoor boundary, however, in situ an air temperature layering might have occurred, especially on the window surface interface. This condition might have slightly varied the air/surface interface boundary condition at the lower and upper part of the frame. In other words, a slight air temperature cooling (below 20 °C) may have occurred in proximity of the floor and a slight temperature increase (above 20 °C) may have occurred in proximity of the ceiling. This layering was neglected by the model.

However, given the small deviations between simulated and measured values, the obtained results were considered admissible for the purpose of the study and the defined frame materials characteristics and boundary conditions were inputted in the building dynamic simulations as discussed in Section 3.3.2.

3.3.2. Building dynamic simulations

The dynamic building simulations were performed in VE (Virtual Environment) from IES (Integrated Environmental Solutions) version 2016.0.0.0.

The building has a condensation boiler (180 kW) that delivers hot water to radiators for a total heated area of ≈ 700 m^2. The boiler does not produce domestic hot water; moreover, no cooling or mechanical ventilation systems are installed in the building. Therefore, the energy performance improvement allowed by each retrofitting scenario, is evaluated in terms of reduction of yearly energy consumption for space heating. From now on defined for brevity energy consumption. For the simulations, historical time series data for Antwerp (year 2013) were used; the heating period is October-April.

The building is characterized by brick masonries, timber ceiling for the first and second floor as well as for the roof and brick and mortar vaults between the basement and ground floor. Preparatory to the building simulations, the thermal performance of two walls, representing the most common masonry typologies, was onsite measured by means of Heat Flow Metering (HFM). Lighting and heating schedule as well as users' schedules were modelled considering the building as usual scenario. Namely considering lighting-hours and typology of lamps and auxiliary equipment according to the offices schedule.

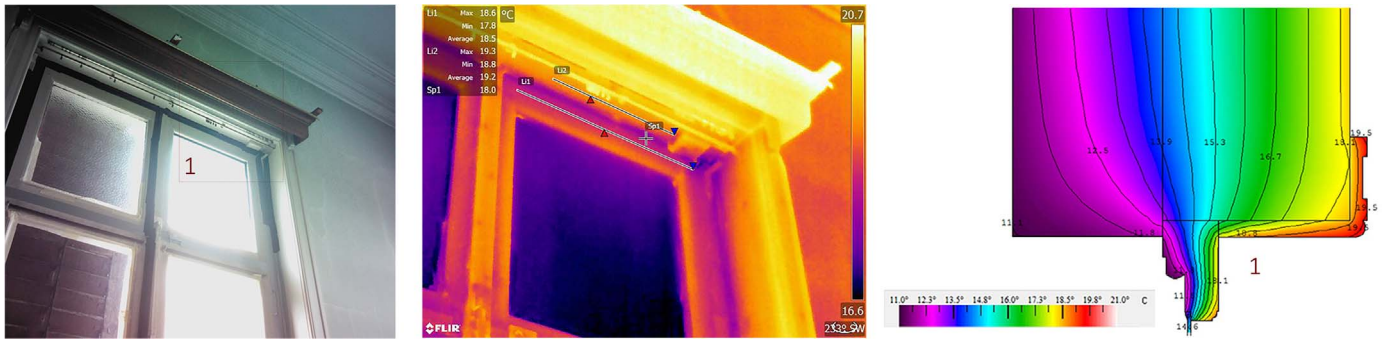

Fig. 3.3.2. (a)–(c) Superior window frame connection; from the left (a) corner localization, (b) IRT imaging, (c) window model (THERM 7.4).

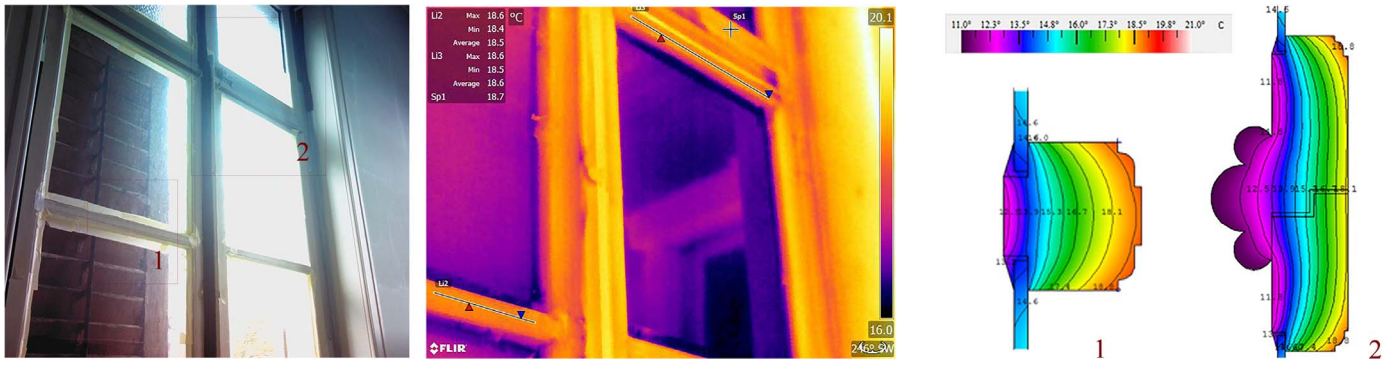

Fig. 3.3.3. (a)–(c) Central window frame connection; from the left (a) transom localization, (b) IRT imaging, (c) window model (THERM 7.4).

For modelling the influence of fenestration deterioration on the building energy consumption, the air infiltration rate measured in space 1 (deteriorated windows) as well as the physical characteristics of the deteriorated windows model discussed in Section 3.3.1, were inputted in the dynamic building model. This first model defines the building baseline (Section 3.5.1). The energy use of the baseline model (scenario 1) describes the consumption the building would have if all the windows would be deteriorated as measured in space 1. This theoretical condition allows retrofitting scenarios results comparison.

An overview of the historic windows geometrical and physical characteristics inputted in the building models for scenarios from 1 to 5 is given in Table 3.3.2.1. Boundary conditions, infiltration rate and additional windows characteristics for all the scenarios are given in Table 3.3.2.2. An overview of the replacement windows physical characteristics inputted in the building models for sub-scenarios 6 is given in Table 3.3.2.3.

For allowing a comparison among windows frame materials and excluding the effect of glazing, in scenarios 5 and 6, an identical Insulating Glass Unit (IGU) double glazed – argon filled was modelled. The IGU initial thermal characteristics – not accounting for the unit technical performance decay – are given in Table 3.3.2.4. The glass centred IGU thermal transmittance value is 1.1 W/m^2 K.

The dynamic building simulations of each scenario were performed considering each perishable component firstly in its initial state (obtaining the initial scenario yearly building energy consumption) and secondly in the deteriorated state (obtaining the decayed scenario yearly building energy consumption). The physical properties of one component per time were adjusted holding the properties of the other components constant at their initial state. This aspect is discussed in the next section.

3.4. Influence of windows technical performance decay on building life cycle operating energy

In order to quantify the windows technical decay, the typical deterioration of the identified perishable components with a bearing on the window energy performance was analysed, see Note 1 in Supplementary material for an extended discussion. Successively, the influence of each component deterioration on the windows technical performance was individually quantified (Table 3.4.1) by using data from onsite measurements and literature research.

Table 3.3.2.1
Boundary conditions and historic windows properties (scenarios 1–5).

Historic windows	Total area (m^2)	Windows percentage of frame (%)	Window thickness (m)	Internal heat laminar flow (W/m^2 K)	External heat laminar flow (W/m^2 K)	Internal frame emissivity (-)	Glass pane SHGC	(Int-Ext) solar transmittance	(Int-Ext) solar reflectance
Basement level	29	40	0.04	7.6	20.6	0.9	0.85	0.82	0.07
Ground level (Type A)	72.9	32	0.04	7.6	20.6	0.9	0.85	0.82	0.07
Ground level (Type B)	32.8	45	0.04	7.6	20.6	0.9	0.85	0.82	0.07
First level (Type A)	70.6	33	0.04	7.6	20.6	0.9	0.85	0.82	0.07
First level (Type B)	13.1	43	0.04	7.6	20.6	0.9	0.85	0.82	0.07
Second level (type A)	7.8	24	0.04	10.13	20.6	0.9	0.85	0.82	0.07
Second level (type B)	4.4	33	0.04	10.13	20.6	0.9	0.85	0.82	0.07

Table 3.3.2.2
Boundary conditions (scenarios 1–6) and windows properties (scenarios 1–6).

Historic windows	η_{nat} (h^{-1}) $\eta_{50}/20$	Historic timber frame thermal conductivity (W/m K)	Glass pane thickness (mm)	Glass pane thermal conductivity (W/m K)
Scenario 1	0.33	0.23	4	1.06
Scenario 2	0.26	0.19	4	1.06
Scenario 3	0.22	0.19	4	1.06
Scenario 4.α/4.γ	0.22	0.19	4/6	1.06
Scenario 5	0.22	0.19	6	1.06
Scenario 6	0.22	–	6	1.06

Table 3.3.2.3
Thermal properties replacement windows frames (scenario 6).

		Mean frame thermal transmittance (W/m^2 K)			Mean frame thermal resistance (m^2 K/W)		
Floor	Window	A	PVC	T	A	PVC	T
−1	A	1.508	1.775	1.400	0.485	0.383	0.53
0	A	1.508	1.775	1.400	0.485	0.383	0.53
	B	1.825	1.833	1.400	0.369	0.369	0.53
1	A	1.508	1.775	1.400	0.485	0.383	0.53
	B	1.825	1.833	1.400	0.369	0.369	0.53
2	A	1.508	1.775	1.400	0.515	0.413	0.56
	B	1.508	1.775	1.400	0.515	0.413	0.56

- Putty on the glass bars; in scenario 2 and 3, the influence of (silicone) putty deterioration was considered in terms of building air infiltration rate alteration. The air infiltration from space 2 (Ƞ26) decays to the one of space 1 (Ƞ33); Section 3.5.2. Because in scenario 4 an internal secondary glazing is present, the putty deterioration of the historic windows is supposed to alter the thermal resistance of the air buffer between the glazing panes but not the building air infiltration rate; see Section 3.5.4. For this reason the deterioration of the putty in scenario 4 is modelled as alteration of the air buffer thermal resistance from the initial (R1) to the deteriorated (R2) state.
- Hydrophobic paint decay; in scenarios 2–5 and 6 (Timber), the deterioration of the hydrophobic paint layer is considered in terms of thermal conductivity alteration of the windows timber frame. The thermal conductivity of the wood in its dry state (λ1) increases to the one of moist state (λ2). Consequentially the frame thermal resistance decreases; see Section 3.5.2.
- Sealant profiles decay; in scenarios 3–6, the influence of sealant profiles around the window sashes and window edges (considered together) was considered, similarly to putty onto glass bars, in terms of building air infiltration rate alteration. The air infiltration from spaces 2 and 1 after the drought proofing (Ƞ22) decays to the one of space 2 (Ƞ26); Section 3.5.3.
- IGU decay; in scenarios 5–6, the influence of the insulating glass unit decay was quantified in terms of argon concentration reduction (from 90% to 66%). The IGU central pane thermal resistance decreased consequentially; see Sections 3.5.5 and 3.5.6.

More information on the typical deterioration of the mentioned perishable components is given in Note 1 in Supplementary material.

3.4.1. Theoretical and methodological assumptions for components deterioration modelling

In this study:

1) the decay of each component is assumed linear and continuous until the component EOL. If the replacement of a given component occurs after the components EOL, the performance of the component does not deteriorate further, see Fig. 3.4.1;

2) the energy saving reduction caused by the deterioration of a given component is independent from the deterioration process of other components. In other words, no interaction between components deterioration is accounted;
3) the non-perishable components, namely components for which the deterioration process other than the breakage is supposed not to influence the window performance, are considered with constant energy performance contribution throughout their service life. These are, aluminium or PVC frame profiles, thermal breaks, low-emissivity coatings and single glass panes.

3.4.2. Analytical procedure for accounting the influence of components deterioration on the building life cycle operating energy

In order to adjust the building life cycle operating energy by taking into account the windows performance decay, a coefficient, termed Yearly Energy Performance Decay Rate (YEPDR) was introduced. This coefficient is calculated once the building energy consumption is obtained from the dynamic simulations considering firstly the perishable components in their initial state and secondly in their deteriorated state; Sections 3.3.2, 3.4 and 3.4.1.

Table 3.3.2.4
Insulating glass unit argon-filled; physical characteristics at the initial state.

Materials (from outside)	Thickness (mm)	Thermal conductivity (W/m K)	Gas (concentration)	Convection coefficient initial state (W/m^2 K)	Thermal resistance -initial state (m^2 K/W)	Outside emissivity	Inside emissivity
clear float	6	1.06	–	–	0.0057	–	–
cavity	16	–	Argon (90%)	1.47	0.6573	–	–
clear float	6	1.06	–	–	0.0057	0.015	–

Table 3.4.1
Components properties variations for accounting the technical decay of windows.

	Putty on glass bars (silicone)	Sealants on window sashes (EPDM + silicone)	Hydrophobic paint layer	Insulating glass unit
scenario 2	Ƞ26 → Ƞ33	–	λ1(0.17) → λ2 (0.21)	–
scenario 3	Ƞ26 → Ƞ33	Ƞ22 → Ƞ26	λ1(0.17) → λ2 (0.21)	–
scenario 4	R1 (air cavity) → R2	Ƞ22 → Ƞ26	λ1(0.17) → λ2 (0.21)	–
scenario 4.γ	R1 (air cavity) → R2	Ƞ22 → Ƞ26	λ1(0.17) → λ2 (0.21)	IGU, argon conc. 90% → 66%
scenario 5	–	Ƞ22 → Ƞ26	λ1(0.17) → λ2 (0.21)	IGU, argon conc. 90% → 66%
scenario 6.A-PVC	–	Ƞ22 → Ƞ26	–	IGU, argon conc. 90% → 66%
scenario 6.T	–	Ƞ22 → Ƞ26	λ1(0.17) → λ2 (0.21)	IGU, argon conc. 90% → 66%

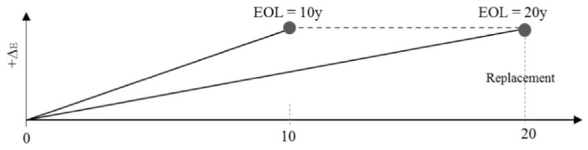

Fig. 3.4.1. Example of decay for a material with 10 and 20 years EOL; material replacement occurs at the 20th year; the term + ΔE, on the y axis, represents the operating energy increase due to the material decay; on the x axis are reported the years.

Table 3.5.1
Description of scenarios and sub-scenarios codification.

Scenarios or sub-scenarios variations	Description	Coding
Scenarios	baseline and improvement scenarios	{1; 2; 3; 4; 5; 6}
Sub-scenarios: frequency	Iteration frequency variations	{.1; .2; .3 … 0.8}
Sub-scenarios: Service Life (SL)	Materials SL variations	{.a; .b}
Sub-scenarios: Technology	Secondary glazing technology variations	{.α; .γ}

YEPDR, represents the yearly building energy saving decrease occurring because of the technical obsolescence of components making up a given assembly. In this study the assemblies are the windows. The YEPDR for the c^{th} component in the a^{th}assembly is determined according to Eq. (2).

$$YEPDR_{a,c} = \frac{(Esav1_{a,c} - Esav2_{a,c})}{SL_{a,c}} \tag{2}$$

where $(Esav2_{a,c})$ is the building Energy saving enabled by the *c*th components in the *a*th assembly after the deterioration process, while $(Esav1_{a,c})$ is the building Energy saving enabled by the *c*th components in the *a*th assembly according to its initial performance. The energy saving loss at the numerator, also definable (Δ_E) is standardised by the component Service Life $(SL_{a,c})$. The maximum yearly energy decay rate from one assembly (a), is given by Eq. (3). Namely by summing up the decay rate of each perishable component making up the assembly.

$$YEPDR_{(a)} = \sum_{c=1}^{n} YEPDR_{(a,c)} \quad c = \overline{1,n} \tag{3}$$

It is worth noting that the Eq. (3) should be calculated singularly for each assembly constituting the retrofitting intervention. In this case for each window. Indeed, different assemblies, may have different Service Life (SL) according to: microclimatic indoor/outdoor conditions, use cycles etc. However, for simplicity, in the present study, we assumed that all the windows follow the same deterioration process, therefore no individual window deterioration is considered. The total YEPDR for all the windows assemblies (YEPDR $_{Total}$), is given by Eq. (4). This coefficient stands for the annual energy saving decrease caused by the decay of all the retrofitting assemblies. If additional retrofitting interventions are included, e.g. wall insulation, roof insulation etc., the total per homogeneous assemblies typology should be calculated.

$$YEPDR_{Total} = \sum_{a=1}^{m} YEPDR_{(a)} \quad a = \overline{1,m} \tag{4}$$

The building energy consumption taking into account each *c*th component technical decay at the *x*th year of the component SL is calculated according to Eq. (5) and defined *Net building energy consumption* (*Ec* $_{net}$).

$$E_{cnet\,(x)} = (E_{1(c)} + (E_{1(c)} \cdot YEPDR_{(Total)}) \cdot (x-1)) \quad x = \overline{1,n} \tag{5}$$

where $(E_{1(c)})$ is the initial energy consumption allowed by the cth component; x is the year of the component Service Life, with n = last year of the component SL. The net cumulative life cycle building energy consumption accounting for the whole assembly technical performance decay is given by Eq. (6). With y = m last year of the building RL.

$$E_{aNet\,(Tot)} = \sum_{y=1}^{n} (E_{1(c)} + (E_{1(c)} * YEPDR_{(a,c)}) \cdot (y-1)) \quad y = \overline{1,m} \tag{6}$$

3.5. Baseline and retrofit scenarios modelling description

With the aim of exploring the life cycle environmental impact variation of the five-fenestration improvement options (see Table 1.1) alongside variations of intervention frequency, technology and materials Service Lives (SLs), each improvement scenario was investigated considering several sub-scenarios. Scenarios and sub-scenarios are discussed in this contribution on basis of the numeration scheme given in Table 3.5.1. The first consequential numbering of the scenarios refer to retrofitting intervention variation, the second order of consequential numbering refers to iteration frequency variation. The coding *a* and *b*

Table 3.5.2
Materials service life (in years).

Service life (SL) perishable (1–4) and not perishable (5) materials						
Scenario	Code	1. Glazing bars putty (silicone)	2. Frame paint (hydrophobic paint)	3. Weather stripping profiles and foam (EPDM-PUR)	4. Insulating glass unit (Argon filled double glass)	5. Window unit
2	a	10	20	–	–	–
3	a	10	20	10	–	–
	b	10	20	20	–	–
4.α	a	10	20	10	–	–
	b	10	20	20	–	–
4.γ	a	10	20	10	25	–
	b	10	20	20	35	–
5	a	–	20	10	25	–
	b	–	20	20	35	–
6.Alu	a	–	–	10	25	50
			–			
			–			
	b	–	–	20	35	50
			–			
			–			
6.PVC	a	–	–	10	25	50
			–			
			–			
	b	–	–	20	35	50
6.Timber	a	–	20	10	25	50
	b	–	20	20	35	50

refers to SL materials variation, while the coding α and γ refers to secondary glazing technology variation (only for scenario 4).

An overview of the activities iteration frequencies performed per scenario and sub-scenario is given in Table 1 in Supplementary material, while a summary of the SLs for the materials considered in this study is given in Table 3.5.2. By considering the activities iteration frequency per scenario, the total number of performed building dynamic simulations was 112. Additionally, 39 simulations were performed for modelling the deteriorated state of the perishable materials, see Section 3.4.

The Service Life of silicone putty is estimated according to onsite acquired information. The deteriorated silicone putty on the glass bars of space 1 was applied over 10 years ago, while it was recently applied in space 2. Therefore, it was assumed silicone putty SL of 10 years.

The technical SL for the high water resistant paint is estimated on basis of literature results. Laboratory test on alkyd and acrylic paints, highlighted that the paint layers undergo plastic deformation and cracking at low air temperature. Mecklenburg in [50] analysed the temperature-induced damage of 20 years-aged alkyd and acrylic paint layers. The author reported that if the temperature lowers beyond the one of glass transition[2] the paint layer experiences plastic deformation and cracking (hence water absorption by the frame). By admitting a simplification and considering that the outdoor average temperature in Belgium is for 6 months a year lower than 10 °C,[3] it is possible to consider that the technical SL of acrylic and alkyd windows paint in outdoor environment is not longer than 20 years. This hypothesis is fully consistent with Life Cycle Assessment (LCA) studies on alkyd emulsion based paints as reported in [51]. It was therefore assumed a technical SL for paint of 20 years.

Also the technical SL for the EPDM weather sealing profiles is estimated on basis of literature review. In the literature it is often reported that EPDM profiles SL may strongly vary according to: temperature cycling, environmental chemical aggressiveness, quality of installation workmanship and profile geometry [52–54]. Considering the variety of the several factors affecting the EPDM SL, two different scenarios were considered according to [54–56]. Sub-scenarios a and b, respectively with SL 10 and 20 years. In the study the sealing materials for the drought proofing (EPDM and silicone) are considered together with EPDM SL.

The technical service life of the IGU, was estimated at 25 years as resulted from laboratory test performed by Garvin in [57]. In the study, the author pointed out the IGU SL might be longer than 25 years depending on environmental circumstances and IGU characteristics such as geometry and material of the spacer and secondary sealing. For taking into account the influence of IGUs durability on the life cycle operating energy of the modelled scenarios, two SL alternatives were considered: alternative a and b respectively 25 years and 35 years.

It is worth mentioning that the SL of non-perishable materials (column 5 in Table 3.5.2) does not influence building operating energy. In this study, the mentioned non-perishable materials are assumed to be replaced together when the window unit is replaced. The replacement frequency of the window units is assumed each 50 years.

3.5.1. Scenario 1: baseline scenario

As mentioned, the baseline building model represents the yearly heating consumption the building would have if all the windows -due to their deterioration- would have infiltration rate equal to the one measured in space 1.

The energy model for scenario 1 was simulated considering the air infiltration rate at 50 Pa measured in space 1 ($\eta_{nat} = 0.33$). Windows thermal properties and boundary conditions are simulated on basis of the results from the calibrated -steady state- windows model. Timber frame thermal conductivity inputted in the calibrated windows model is 0.23 W/m K. This value, also inputted in the building dynamic model for scenario 1 (Table 3.3.2.1), corresponds to the conductivity of "moist hardwood, oak" in Table 3.39 in CIBSE, Guide A [49].

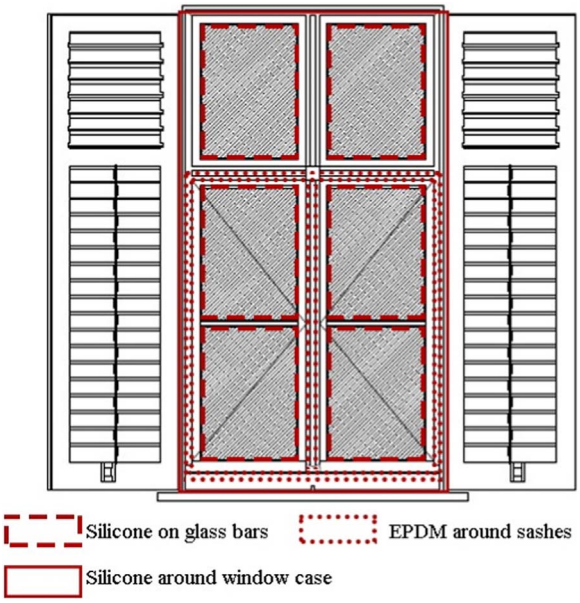

Fig. 3.5.3.1. Localization of the silicone-putty on the window sashes glass bars (scenario 2), EPDM sealing profiles on the sashes and silicone around the window edges (scenario 3).

3.5.2. Scenario 2: fenestration maintenance

Even if windows maintenance is generally not included among the activities aimed at reducing buildings energy demand, this study analysed the extent to which its implementation permits reduction of infiltration and conductive losses, hence, to improve the overall building energy efficiency. It is worth mentioning that, windows maintenance only allows to regain the energy performance the building was supposed to have in its initial state. Additional savings can only be obtained if implementing energy retrofitting interventions [58,59].

Windows maintenance activities considered in this study are: replacement of the glass bars putty, windows painting and ironmongery oiling. Putty replacement allows for a reduction of the infiltrative losses, while window painting indirectly allows for a reduction of the conductive losses. The position of the silicone putty onto the glass bars is represented in Fig. 3.5.3.1 in the next section.

The energy model for scenario 2 was simulated considering the air infiltration rate measured in space 2 ($\eta_{nat} = 0.26$). The underlying hypothesis is that after the restoration and maintenance of building fenestration, the infiltration rate as measured in space 2 is obtained in all the building spaces.

After maintenance, it is assumed that timber windows frame equilibrium moisture content reduces because of the application of high water resistance coating [60]. The timber frame thermal conductivity is assumed to drop from 0.23 to 0.19 W/m K; namely from moist to dry hard wood in Table 3.39 in CIBSE, Guide A [49]. Consequentially the timber frame thermal Resistance (R) increases from 0.17 to 0.21 m^2/W K.

In scenario 2, the considered perishable materials are: water vapour resistance paint coating and silicone-based putty on the glass bars. For quantifying the individual energy saving fraction attributable to the silicone putty onto the glass bars and to the hydrophobic paint layer, the individual energy saving contribution allowed by both the materials, was individually simulated. As that total energy saving resulting

[2] Temperature of glass transition was found between 10 °C and 7.22 °C for Alkyd paint and 4.44–1.66 °C for Acrylic paint; pag. 15 in [50].

[3] From https://www.worldweatheronline.com/brussels-weather-averages/be.aspx; acceded on 24/05/2017.

from the independent simulation of each single intervention was larger than the one obtained by the simultaneous interventions simulation, the energy savings were standardised. This standardisation was performed in each scenario.

This study considers the hypothesis that, at the end of the paint layer SL, the timber frame thermal conductivity goes back to the stage pre-maintenance (R from 0.21 to 0.17 W/m K). Moreover, at the end of the silicone putty SL, the building infiltration level goes back to the value pre-glass bars maintenance (η_{nat} from 0.26 to 0.33). No residual energy saving is allowed by silicone putty or paint layer at the end of their SL.

3.5.3. Scenario 3: fenestration drought proofing

In scenario 3, additionally to the windows maintenance activities described in scenario 2, the windows drought proofing was modelled. The drought proofing consisted in EPDM profiles on windows sashes and silicone on the windows (fixed frame) edges. The position of the air – drought proofing sealants (EPDM profiles and silicone) as well as the one of the silicone putty on the glass bars (from scenario 2) is shown in Fig. 3.5.3.1.

Beside being among the less invasive windows retrofitting options, windows weather-stripping is considered an effective intervention for improving energy efficiency especially of historic fenestration [61,62].

The energy model for scenario 3 was simulated considering the mean air infiltration rate at 50 Pa measured in space 1 and 2 after the drought proofing (η_{nat} = 0.22). The underlying hypothesis is that after the maintenance and drought proofing of the building fenestration, the infiltration rate as measured in space 1 and 2 after the draught proofing is obtained in all the building spaces. We considered the sealing materials (EPDM and silicone around the edges) as unique material. The study considers the hypothesis that, at the end of the sealing materials SL, the building infiltration level goes back to the value pre-drought proofing and not to the non-maintained windows ($\eta_{nat}$from 0.22 to 0.26).

3.5.4. Scenario 4: internal storm glazing addition

The literature, often reports the usefulness of adding a secondary glazing (also termed storm glazing) on the inner or outer side of an existing window as alternative option to glass or window replacement [63–65]. This alternative is especially valid in case of historic buildings as their operating energy can be reduced without threatening the existing fenestration [2,7,8,61,66].

In this study, additionally to the contribution given by fenestration maintenance and drought-proofing (scenario 2 and 3), it was quantified the extra contribution given by the addition of an internal – inwards operable- secondary glazing, see Fig. 3.5.4.1.

In order to avoid turbulent air motion with consequent increase of convective losses, the air buffer between the existing window glass pane and the one of the inner glazing, is generally recommended between 50 and 60 mm [7].

However, in the present case study, due to the geometry of the existing windows handle, it was not possible to respect this geometrical requirement. In the modelled scenario, the maximum distance between existing and secondary frame is 120 mm while the maximum distance between glass panes is 168 mm. The internal storm glazing is connected to the building masonry via a timber counter frame. The counter frame, beside increasing the secondary glazing stability, allows visual alignment with the historic windows.

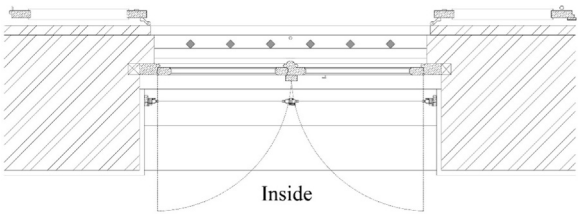

Fig. 3.5.4.1. Horizontal section window basement level; secondary glazing alternative 4.α.

In order to obtain results representative of the most applied secondary glazing technologies, two sub-scenarios were simulated: scenario 4.α refers to the installation of a single-glazed secondary glazing and scenario 4.γ refers to a double-glazed argon-filled secondary glazing.

As mentioned in Section 2, the aluminium frame and the single glass pane are not considered subjected to decay. For this reason, the materials subject to technical decay in sub scenarios 4.α are identical to scenario 3, namely EPDM sealant profiles and silicone glass putty. While in sub-scenario 4.γ, is the IGU performance decay caused by the reduction of the volumetric argon concentration into the cavity also calculated; see Note 2 in Supplementary material for details.

The energy model for scenario 4 was simulated considering the mean air infiltration rate at 50 Pa measured in space 1 and 2 after the drought proofing (η_{nat} = 0.22). It is worth mentioning that, the internal secondary glazing does not enable air tightness reduction beyond scenario 3. Indeed, drought-proofing of the historic fenestration also performed in scenario 4 (see Table 1.1), allows by itself the maximum air tightening achievable by intervening on the building fenestration. Therefore, from scenario 4 onwards, any extra- increase of building energy saving is attributable to the reduction of windows conductive losses.

The heat transfer through the window (existing window – still air into the cavity – secondary glazing) was modelled according to EN 673.2011 [67] as described in Note 2 in Supplementary material. Initial air buffer thermal resistance was, hence, determined.

Because of the wide thickness of the air gap, it was necessary to verify the absence of convection into the cavity. In other words, it was necessary to confirm that the heat transfer into the cavity occurs via conduction and possibly only via convection. The increase of convection, indeed, may unavoidably decrease the air gap thermal resistance and generate air turbulences within the gap. With this purpose, the *Nusselt* number (N_u) was calculated. For the physical background of (*Nu*), refer to [67,68] and for its calculation procedure see Note 2 in Supplementary material. Steady state window simulations in THERM were run in order to evaluate the heat flow path (especially at the materials connection) and the air temperature distribution before and after the intervention.

The *Nusselt* number (*Nu*), calculated considering the calibrated window model (see Tables 1 and 2 in Note 3 in Supplementary material), was respectively ≈ 0.72 and ≈ 1.17 for vertical windows and (inclined) skylights.

The obtained results showed that the heat transfer through the windows occurs via conduction for the vertical windows and with a slight convective contribution for the skylights. The initial air buffer thermal conductance (not accounting for the materials decay) considering the initial boundary conditions and (*Nu*), resulted 0.150 and 0.175 W/m^{2}K respectively for vertical windows and inclined skylights.

Further, was foreseen the influence of the sealants deterioration of the historic (drought-proofed) window and the one of the internal secondary glazing. In the study, we assumed that the deterioration of the sealant on the historic windows causes the alteration of the air thermal resistance inside the air buffer, while the deterioration of the sealant of the secondary glazing causes the increase of the building infiltration rate. However, these circumstances occur simultaneously, therefore, their influence on the operating energy alteration is cumulative.

In case the sealants on the historic windows deteriorate (EPDM profiles and silicone putty), the air buffer is no longer airtight, consequently the thermal resistance of the air buffer reduces because of the increased convection (increased *Nu*). Simultaneously, since the sealant on the secondary glazing deteriorates (EPDM profiles), the infiltration

Table 3.5.4.1
Calculation of initial and decayed air buffer thermal resistance (R); initial (R1), calculated according to EN 673.2011 and decayed (R2), calculated according to EN ISO 6946. Hypotized fissure glass putty area 5.1 cm^2.

Floor	Window	Window glass putty area -external side (mm^2)	Window length (m)	Fissure area (mm^2)	*Av* (mm^2)	Initial R air cavity (m^2 K/W)	Decayed R air cavity (m^2 K/W)	Rt reduction (%)
−1	A	581.28	1.53	501	766.53	0.260	0.205	−0.21
0	A	1240.00	1.53	501	766.53	0.260	0.205	−0.21
	B	1270.00	1.84	501	921.84	0.260	0.173	−0.33
1	A	1436.00	1.54	501	771.54	0.260	0.204	−0.22
	B	1755.00	1.43	501	716.43	0.260	0.215	−0.17
2	A	1261.00		501	661.32	0.258	0.225	−0.13
	B[a]	351.00		501	501	0.258	0.258	0.00

[a] The surface area of this skylights was considered 1 m^2 instead of 0.75 m^2 for avoiding inconsistency within the calculation (see EN 673.2011).

Table 3.5.4.2
Insulating glass unit argon-filled; physical characteristics before and after technical performance decay.

Materials (from outside)	Thickness (mm)	Thermal conductivity (W/m K)	Gas (concentration initial → decayed)	Convection coefficient initial state (W/m^2 K)	Convection coefficient decayed state (W/m^2 K)	Thermal resistance -initial state (m^2 K/W)	Thermal resistance -decayed state (m^2 K/W)	Outside emissivity	Inside emissivity
clear float	6	1.06	–	–	–	0.0057	0.0057	–	–
cavity	16	–	Argon 90% → 66%	1.47	1.63	0.6573	0.5859	–	–
clear float	6	1.06	–	–	–	0.0057	0.0057	0.015	–

rate in the building goes back to a value pre-drought proofing state (η_{nat} = 0.26).

To quantify the influence of the sealants deterioration (e.g., deformation, detachment etc.) on the reduction of the entire window thermal performance, the decrease of the air buffer thermal resistance due to the presence of a hypothetical 5.1 cm^2 fissure area on the sealants of the historic windows in accordance to EN 6946 [48] was calculated; see Note 4 in Supplementary material.

Due to the air infiltration, the air buffer -unventilated in its initial state- becomes slightly ventilated. The thermal resistance of the air gap reduces by up to 30% compared to its initial value; see Table 3.5.4.1. It is worth noting that, the air buffer thermal resistance does not reduce to zero because of the passive behaviour of the internal glazing. There is still residual energy saving after the perishable components EOL.

With regard to scenario 4.γ, not only the possible thermal performance decay of the sealing profiles of both historic windows and secondary glazing was calculated, but also the decay of the gas volumetric concentration into the IGU. In the study we considered that the initial IGU gas volumetric concentration is 90% [69]. Further, by considering a maximum yearly gas leakage rate of 1%/y as allowed by the EN 1279-3.2012 [70], the argon volumetric concentration at the end of the IGU SL, reduced to 65.36%, rounded to 66%. The volumetric gas concentration loss hypotized over the IGU SL is consistent with laboratory test results reported in Table 2 in [71]. On this basis the 16 mm argon cavity convection coefficient, hence the IGU thermal resistance in its initial and deteriorated state was calculated and inputted in the dynamic simulation models, see Table 3.5.4.2. The calculation followed the specifications in EN 1279-3 [70] reported in Note 5 in Supplementary material. The gas properties of the initial and final gas-mixture within the IGU cavity as well as the IGU thermal properties are calculated according to the procedure in §6.2 in EN 673.2011 (E) [67] reported in Note 6 in Supplementary material.

3.5.5. Scenario 5: glass pane replacement

Another widely diffused intervention for historic windows is the substitution of the glass panes and the retention of the window frame [2,7,62,72]. Because this intervention is generally targeted at reducing the conduction losses of the fenestration, the glass panes are often replaced by IGU, usually with low emissivity coatings [2]. An additional heat loss reduction can be achieved if, like in the presented case, the

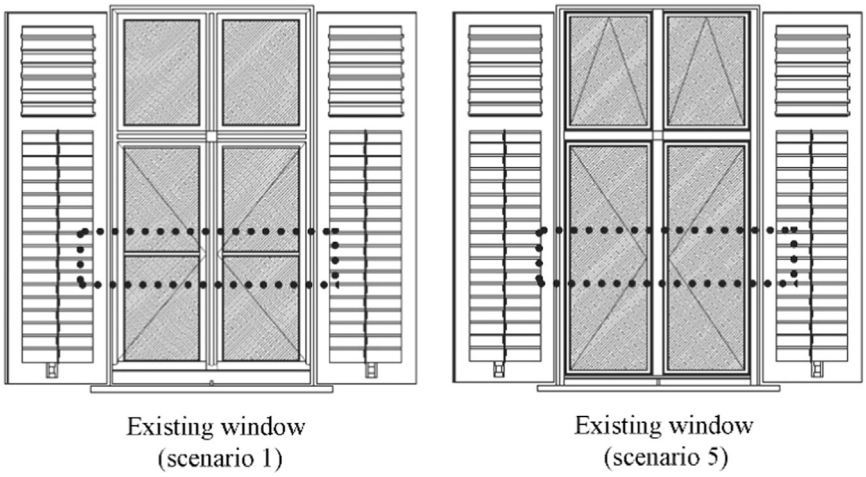

Fig. 3.5.5.1. Front view of existing window at the first floor (type A) in its existing state and after the implementation of scenario 5; the dotted rectangle localises the removed glass bars.

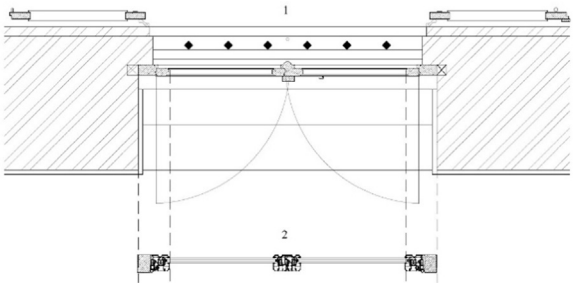

Fig. 3.5.6.1. Plan view of existing window at the basement level (1) and example of (aluminium) replacement window with timber sub frame (2); the dotted line indicates visual profiles alignment.

glass pane replacement is combined with windows maintenance and drought-proofing. However, because the replacement of a single glass pane with an Insulating Glass Unit, IGU may increase up to 4 times the sashes weight [61], the consolidation of the timber frame should be not neglected. Nevertheless, since windows restorations plays a driving role only on the embodied impacts, it is not discussed in this article.

The energy model for scenario 5 was simulated considering the mean air infiltration rate at 50 Pa measured in space 1 and 2 after the drought proofing (η_{nat} = 0.22). The windows were modelled considering the IGU physical characteristics already given in Table 3.5.4.2 and the physical characteristics of the maintained and drought proofed existing window frames already given in Tables 3.3.2.1 and 3.3.2.2.

The windows technical decay, in this case, is attributable to the paint deterioration on the historic timber frame, EPDM sealing profiles on the sashes, silicone decay around the windows edges and gas volumetric concentration reduction into the IGU. Differently from the previous scenarios, the decay of the silicone putty on the glass bars is no longer included because the multiple glass panes making up the existing sashes are replaced by only one IGU per sash, Fig. 3.5.5.1.

3.5.6. Scenario 6: windows replacement

In scenario 6, the total fenestration replacement is simulated. The historic windows are replaced by aluminium, PVC or timber windows. In this study, replacement windows are installed without varying the outer visual alignment of the existing window frames. The alignment is allowed by introducing a few centimetres timber studs if the replacement frame is smaller than the existing one; see Fig. 3.5.6.1.

In order to obtain results representative of standard aluminium, PVC or timber products, the mentioned replacement windows, were modelled considering the mean geometric and physical characteristics of three different products per window typology. Timber windows were modelled only considering data from one EU producer. The window replacement frames, had mean profile dimension of 10 cm ± 1.5 cm height, and 7.5 ± 1 cm width. The mean frame thermal transmittance value for the three technologies are given in Table 3.3.2.3. The double glazing IGU foreseen in each window replacement option is the same as the one modelled in scenario 4.γ and 5.

The energy model for scenario 6 (all alternatives) was simulated considering the mean air infiltration rate at 50 Pa measured in space 1 and 2 after the drought proofing (η_{nat} = 0.22). The windows technical decay, in this case, is attributable to: EPDM sealing profiles on the sashes, silicone decay around the windows edges, gas volumetric concentration reduction into the IGU and (for scenario 6.T) paint layer decay.

Table 4.1
Scenarios energy consumption in initial (E1) and decayed state (E2).

Scenario	Standardized initial heating consumption (kW h)	Standardized residual heating consumption (kW h)
_scenario 1	182,120.45	182,120.45
_scenario 2	174,187.28	182,120.45
_scenario 3	170,389.22	175,521.51
_scenario 4.α	142,633.28	150,746.29
_scenario 4.γ	139,928.70	146,237.06
_scenario 5	143,304.44	149,206.07
_scenario 6-alum	138,540.04	143,723.28
_scenario 6-PVC	139,564.04	145,172.13
_scenario 6-Timber	137,715.86	148,536.80

4. Baseline and retrofit scenarios results

The standardized initial and residual energy consumption with regard to each scenario is given in Table 4.1 and related energy savings are shown in Fig. 4.1. It is worth mentioning that the energy savings discussed in this section, do not include either the intervention iteration frequency nor the materials durability. Therefore, it only represents the initial and residual energy savings of each scenario modelled in its initial and deteriorated state, but it does not represent the building life cycle operating energy saving over the considered 100 years Reference Life. The latter will be discussed in Sections 4.1–4.6.

From the results it can be seen that performing simple building maintenance (scenario 2), is a practice that allows in itself building energy performance improvement. In the specific case, building energy demand was reduced by up to ≈ 4.40%. More specifically the re-putty of the glass bars and the re-painting of the timber frames allowed reducing energy consumption by up to 3.63% and 0.76% respectively; see Table 4.2. However, due to silicone and paint layer deterioration, the obtained saving are likely to be lost at the end of the materials SL.

If window maintenance is combined with windows drought proofing (scenario 3), namely with the addition of sealing profiles around the sashes and at the edges of the fixed frame, the initial energy saving may increase up to 6.44%. The application of putty onto the glass bars and paint onto the window frame allow respectively 2.32% and 0.46% initial energy saving, while the air-sealing of sashes and fixed frame, allows additional 3.66% energy saving; Table 4.2. At the end of the sealants SL, in accordance to the hypothesis formulated in Section 3.5.3, the fenestration goes back to a performance state prior to the drought proofing allowing a residual energy saving of 3.63%. In other words, 56.35% of the initial saving is still present at the end of the perishable components end of life; see Table 4.3.

If all the scenarios are compared, considering their initial and residual energy saving, it can be seen that aluminium and PVC replacement windows (scenarios 6.A and 6.PVC) allow for the largest savings among the investigated ones; 84.37% and 82.80% energy saving are still respectively present also after the components deterioration; see Table 4.3. Obviously, this occurs because of the relative small technical decay of their perishable components.

The initial energy saving allowed by scenarios 6.A and 6.PVC, is respectively 23.93% and 23.37%, while the residual energy saving is respectively 20.19% and 19.35%. The largest among the investigated scenarios; see Fig. 4.1 and Table 4.2. The initial energy savings allowed by aluminium or PVC replacement windows is attributable to the IGU (17.42% and 17.86% for scenarios 6.A and 6.PVC), to the frame (3.87% and 2.84% for scenarios 6.A and 6.PVC) and to the sealing profiles (2.63% and 2.67% for scenarios 6.A and 6.PVC). As mentioned in Section 3.5.6, for both the scenarios, the technical performance decay is attributable to the deterioration of the windows sealants and IGU, see Table 4.2.

With regard to the timber replacement window (scenario 6.T), there are other considerations. Although this intervention enables the highest initial energy savings (24.38%), it finally results in low residual savings (16.52%) at the end of the components SL, see Table 4.2 and Fig. 4.1. Among the modelled retrofitting alternatives, hence excluding windows maintenance, scenario 6.T has the lowest residual energy saving ratio (67.77%) see Table 4.3. This occurs due to the large fraction of

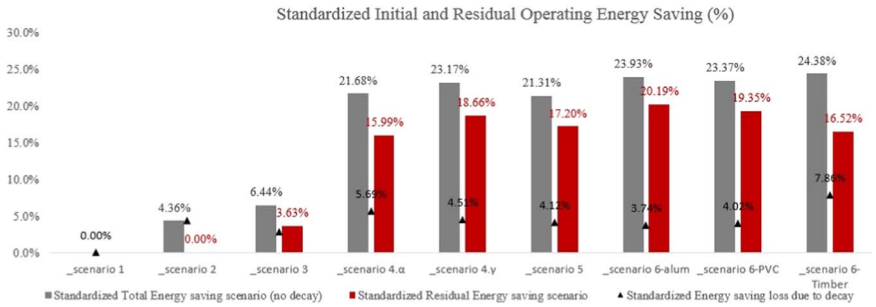

Fig. 4.1. Initial and residual operating energy saving (before and after the materials decay); not accounting for scenario iteration frequency and materials durability.

Table 4.2
Break down standardized energy saving fractions per considered window components and initial-residual standardized Energy savings.

	Std. energy saving from silicone putty	Std. energy saving from hydrophobic paint	Std. energy saving from EPDM weather stripping profiles	Std. energy saving from single glass unit	Std. energy saving from insulating glass unit		Std. energy saving from window frame	Std. total energy saving Initial	Std. energy saving loss	Std. total energy saving residual
					Initial	Residual				
scenario 1									0.00%	
scenario 2	3.63%	0.73%						4.36%	4.36%	0.00%
scenario 3	2.32%	0.46%	3.66%					6.44%	2.81%	3.63%
scenario 4.α	2.09%	1.29%	2.31%	15.99%				21.68%	5.69%	15.99%
scenario 4.γ	0.87%	1.03%	1.88%	15.99%	3.40%	2.66%		23.17%	4.51%	18.66%
scenario 5		1.11%	2.11%		18.09%	17.20%		21.31%	4.12%	17.20%
scenario 6-alum			2.63%		17.42%	16.32%	3.87%	23.93%	3.74%	20.19%
scenario 6-PVC			2.67%		17.86%	16.51%	2.84%	23.37%	4.02%	19.35%
scenario 6-Timber		3.86%	2.61%		17.92%	16.52%		24.38%	7.86%	16.52%

Table 4.3
Energy saving ratio (ratio between residual and initial energy saving.

Scenarios	Scenario 3	Scenario 4.α	Scenario 4.γ	Scenario 5	Scenario 6-alum	Scenario 6-PVC	Scenario 6-Timber
Energy Saving Ratio (Residual/Initial)	56.35%	73.77%	80.54%	80.68%	84.37%	82.80%	67.77%

technical decay (7.86%). Indeed, the deterioration of the paint layer (3.86%) causes the timber thermal conductivity to increase to the one of moist timber (Table 3.4.1). Additionally window sealants and IGU, cause the initial energy saving to decay of respectively 2.61% and 1.39%.

The application of an internal double-glazed secondary glazing (scenario 4.γ) or also the replacement of the existing single glazing with a double-glazed IGU (scenario 5) allows larger residual energy savings ratio than replacing the existing windows with timber units (scenario 6.T). Indeed, with regard to these scenarios, from the initial savings, still 80.54% and 80.68% energy reduction is viable after the components deterioration; see Table 4.3. Also the installation of a single glazed storm glazing (scenario 4.α) results in higher residual energy saving ratio (73.77%) than the ones obtained by scenario 6.T. Nevertheless, the absolute residual energy saving is lower than the one allowed by scenario 6.T.

Scenarios 4, allows larger energy saving than scenario 5. This because of the combined effect of air buffer and indoor glass pane. Indeed, scenario 5 allows 21.31% initial energy saving while scenarios 4.α and 4.γ respectively 21.68% and 23.17%. However, in scenario 4.α, the decay of the historic windows sealing materials cause the thermal resistance of the air cavity to decrease. The residual energy saving goes below the one of scenario 5. Conversely, the residual energy savings for sub-scenario 4.γ (18.66%) is still higher than the one of scenario 5 after the technical decay. This occurs because the conductive losses reduction (allowed by the presence of air cavity and internal secondary glazing with IGU) is large despite the technical deterioration. In other words in this case the passive contribution of the air buffer, cumulates with the one of the IGU.

As mentioned at the beginning of the section, the results until now discussed, do not consider both scenarios iteration frequency and materials durability. Hence the effect of time is neglected.

Although this would be the end of EERI analysis according to the current assessment methodologies present in the Literature, it is limitative if not misleading to draw conclusions about EERI effectiveness on basis of this static assessment approach. This, not only because arguing about technical performance decay without relating it to a time frame is unrealistic, but also because several interventions may be performed in different moments of the building Reference Life, generating a variation of the LC operating energy savings. These aspects will be discussed in Sections 4.1–4.6.

4.1. Scenario 1 results: baseline scenario

Scenario 1, simulated the building with no-maintained fenestration. The resulting annual energy consumption for heating is 182,120.45 kW h. If the fenestration state of conservation were to stay as the one measured in space 1 -without further deterioration – the life cycle operating energy at the end of the considered RL will be 18,212,044.92 kW h; see Table 2 in Supplementary material.

4.2. Scenario 2 results: fenestration maintenance

In the present case study, the implementation of basic windows maintenance reduced by 21% the building infiltration rate resulting in ≈ 4.40% initial energy saving compared to scenario 1. The (initial) building energy consumption decreased from 182,120.45 to 174,187.28 kW h.

Since the energy saving allowable by windows maintenance also depends on the state of conservation of the building, even higher results can be obtained [7,61]. Beside the benefits in terms of energy consumption reduction, window maintenance allows the elongation of the historic windows SL. Maintained windows indeed, can even survive the life time of the building itself [8,73,74].

Since the long-term energy saving benefit of building maintenance depends upon the frequency of its iteration, three different sub-scenarios are modelled considering fenestration maintenance frequency of 5, 10 and 15 years. Respectively defined sub-scenario 2.1, 2.2 and 2.3, see Table 1 in Supplementary material.

Performing window maintenance each 5, 10 and 15 years allows achieving respectively 3.56%, 2.56% and 1.88% life cycle operating energy reduction at the end of the considered building RL; see Table 2 in Supplementary material.

Fig. 9 in Supplementary material shows the life cycle operating energy variation consequent to the implementation of the three sub-scenarios. In the figure, with regard to sub-scenario 2.3 (maintenance iterated each 15 years), it can be seen that the slope of the yearly performance decay varies from the 10th year. This occurs because from the 10th year, the only perishable component until the intervention iteration is the paint (paint has 20 years SL); silicone putty has already reached its End of SL, hence it does not further deteriorate, Section 3.4.

4.3. Scenario 3 results: fenestration drought proofing

In the present case study, according to the results from the onsite performed BDT (see Section 3.2), the windows draught proofing, allowed 16% ACH reduction in addition to the maintained windows and 37% in comparison with the non-maintained windows. This resulted in additional 2.09% initial energy saving allowed by windows drought proofing in comparison with windows maintenance and 6.44% energy saving in comparison with no windows maintenance. Fenestration drought proofing was performed additionally to fenestration maintenance as generally undertaken in the daily practice [61].

In all the iterations foreseen in scenario 3, see Table 1 in Supplementary material, windows maintenance is always preparatory to windows drought proofing. In the specific case windows drought proofing consisted in installing weather stripping (EPDM) profiles around the sashes and sealing with silicone the window edges in connection with sills and jambs (see Fig. 6–8 in Supplementary material). The intervention allowed to reduce the initial building yearly consumption from 182,120.45 to 170,389.22 kW h. The life cycle operating energy for the scenario 3 alternatives is reported in Table 2 in Supplementary material.

As already mentioned for windows maintenance, also windows drought proofing has different effectiveness depending on the windows state of conservation. In a study from Pickles et al., the historic windows weather-stripping allowed air infiltration reduction by 86%, far larger than 37% obtained in the present study [7]. However, nothing is known about the influence of this reduction on the building energy consumption reduction.

Scenario 3, modelled seven sub-scenarios considering for each one a variation of maintenance and drought proofing iteration frequency. More specifically it was modelled a maintenance frequency of 5 and 10 years (the most effective from scenario 2) combined with a drought proofing iteration frequency of 5,10,20,30 years; see Table 1 in Supplementary material. Further, each sub-scenario was modelled considering two materials SL alternatives (Table 3.5.2) resulting in 14 sub-scenarios.

In this scenario, the sole difference between alternatives a) and b) concerns the sealants (EPDM and silicone around the edges), considered with 10 and 20 years SL: respectively alternative a) and b). Nevertheless, in the specific case, because of the low technical decay of the sealants, the influence of their durability is negligible. Indeed, if considering the use of weather stripping profiles with 20 years SL instead of 10, the additional operating energy saving is only 0.01% at the end of the building SRL (maximum difference of savings between alternatives a and b among the 14 alternatives).

In other words, although it appears clear that materials durability contributes to increase building life cycle operating energy savings, in this scenario the contribution is negligible because the perishable fraction of the energy savings allocable to the weather stripping profiles is negligible. The energy saving loss attributable to the weather stripping profiles deterioration in scenario 3 is 0.03%; see Table 4.2.

The mentioned condition makes the proposed scenario 3 alternatives extremely similar from an energy saving point of view, see Fig. 10 in Supplementary material. The operating energy saving among the 14 alternatives range between 5.27% and 5.93%, and Tables 1 and 2 in Supplementary material.

4.4. Scenario 4 results: internal storm glazing addition

In the present case study, the addition of a secondary glazing from the inner side of the historic fenestration allowed an initial energy consumption reduction from 182,120.45 to 142,633.28 kW h in case of a single glazed secondary glazing (scenario 4.α) and to 139,929.70 kW h in case of a double glazed IGU argon-filled secondary glazing.

As distinct from the measures so far discussed, the installation of a secondary glazing allowed not only to reduce the infiltrative losses, but also the conductive ones. Consequentially, the surface temperature of the internal glass pane slightly increased after the introduction of the secondary glazing, while the outer glass pane reduced in comparison with the current situation. Fig. 4.4.1 shows the comparison between surface temperature distribution in the current window (scenario 1) and after the installation of an internal single-glazed secondary glazing (scenario 4.α). If considering the calibrated window model and boundary conditions already discussed in Section 3.3.1, it can be observed that the internal glass pane surface temperature increased by up to 1.1 °C and the historic window glass pane decreased by up to 3 °C. It can be hence supposed that the implementation of scenario 4, even if considering the less performing alternative 4.α, would likely generate an improvement of the indoor building microclimate quality. However, as this aspect is not object of the present study, it is not further discussed.

Scenario 4 (alternative α and γ), includes all the activities of scenario 2 and 3 as discussed in the previous sections; see Table 1 in Supplementary material and Figs. 11 and 12 in Supplementary material.

In Table 1 in Supplementary material the iteration frequency for all the activities to be undertaken in scenario 4 are reported; the considered components SL are given in Table 3.5.2. In total, 14 alternatives for scenario 4.α and 16 for scenario 4.γ. The two additional alternatives from scenario 4.γ refer to the SL of the Insulating Glass Unit.

For completeness Table 3.5.2 reports the SL of the aluminium secondary glazing window frame. However, as mentioned, this component does not have any influence on the life cycle building operating energy variation as no technical decay was assumed; see Section 3.2. Also the single glass pane is supposed not to encounter technical obsolescence. Therefore, in scenarios 4.α and 4.γ, the components subject to decay are identical to scenarios 2 and 3 with the only addition of the IGU in case of scenario 4.γ.

The alternatives concerning the materials SL variation, refer to the IGU and sealing materials (EPDM and silicone around the window

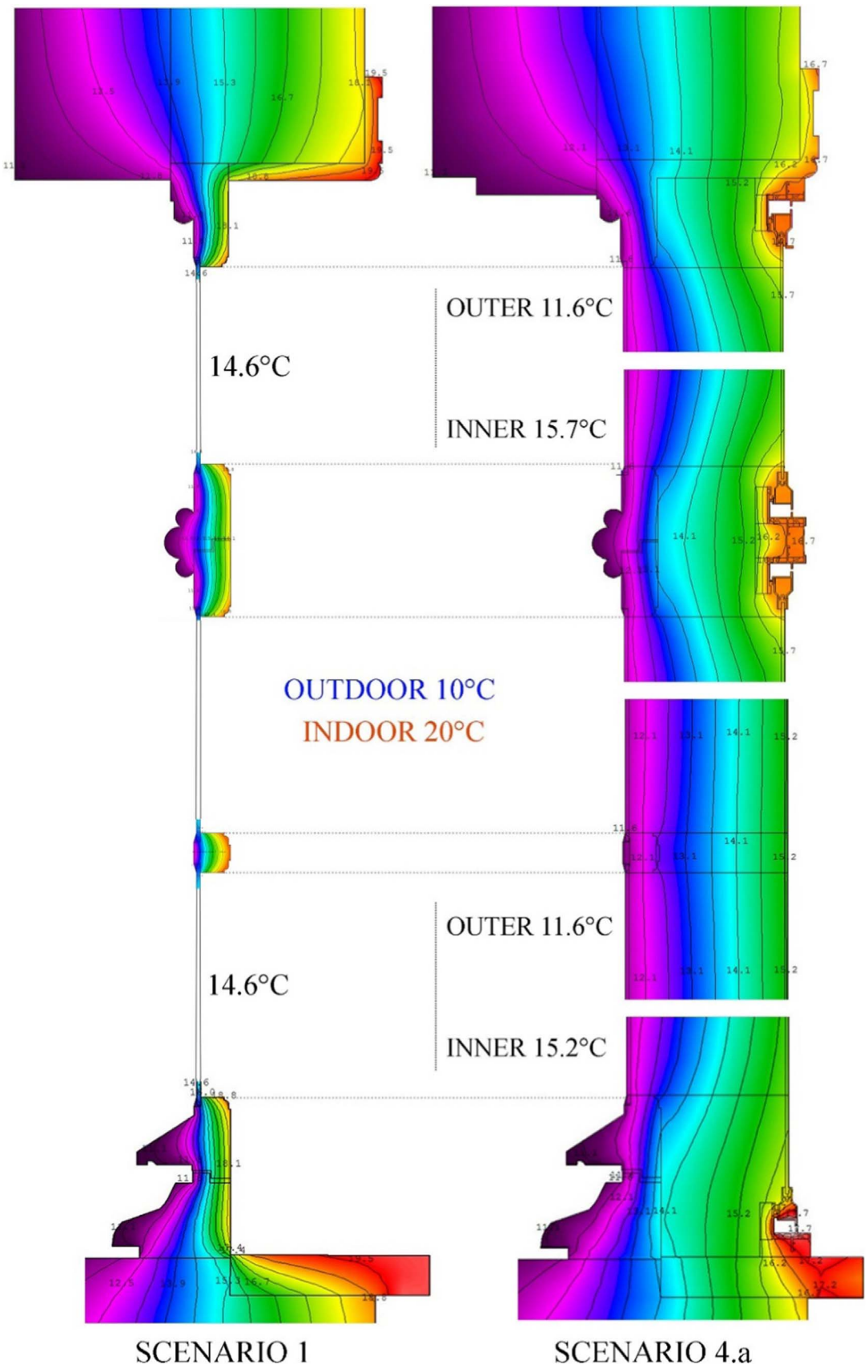

Fig. 4.4.1. Windows A ground floor in its initial state (scenario 1) and after the installation of a single glazed secondary glazing (scenario 4.α).

edges). More specifically, the IGU is modelled with 25 and 35 years SL in alternative a) and b) respectively. While sealants are modelled respectively with 10 and 20 years SL in alternative a) and b) respectively.

The life cycle operating energy savings allowed by scenario 4.α at the end of the considered building RL, range between 18.65% and 20.90%, while the ones allowed by scenario 4.γ, range between 20.54% and 22.45%.

The first consideration looking at the most effective alternatives between sub-scenarios α and γ is that, the installation of an internal secondary glazing with double glazed argon-filled unit instead of a single glass pane, allows to reach maximum 1.55% additional energy saving at the end of the 100 years. The maximum saving for scenario 4.γ is allowed by sub-scenario 4.8.b (see Table 2 in Supplementary material); while for scenario 4.α it is allowed by sub-scenario 4.7.b. Both the scenarios refer to alternative b) meaning that in both the cases the most effective alternative is the one with durable materials.

Within alternatives 4.α.7.b and 4.γ.8.b, all the activities iterations and materials SL are identical (see Table 1 in Supplementary material and Table 3.5.2), the only difference is the use of a durable IGU with 35 years SL replaced each 25 years instead of a single glazing replaced each 50 years. Therefore, it can be concluded that the installation of a durable IGU instead of a single glass, yields to an extra saving 1.55% operating energy in 100 years.

This maximum extra energy saving reduces to 1.26% if considering an IGU with 25 years SL replaced each 25 years (sub-scenario 4.γ.8.a) and reduces to 1.07% if considering an IGU with 25 years SL replaced each 50 years (sub-scenario 4.γ.7.a). In the latter case, if extending the IGU SL from 25 to 35 years, the extra energy saving increases to 1.33% (sub-scenario 4.γ.7.b).

According to the introduced methodology for considering the influence of materials durability into the life cycle operating energy variation (see Section 3.4), a longer materials SL results in larger energy saving. However, the increase of energy saving depends on the ratio between energy saving fraction given by the specific components and its service life and obviously on the replacement frequency.

In all the modelled cases, the selection of materials with longer service life enabled additional operating energy saving. In scenario 4.α, the use of sealants profiles with longer SL (20 years instead of 10) allowed up to 1.06% additional savings at the end of the considered building RL. In scenario 4.γ, the installation of an IGU with longer SL (35 years instead of 25), allowed additional saving up to 0.57%.

4.5. Scenario 5 results: glass pane replacement

In the present study, the replacement of the existing single glazed with a double-glazed argon filled IGU, allowed an initial energy consumption reduction from 182,120.45 to 143,304.44 kW h.

In this scenario the existing windows frame is kept onsite and adjusted in order to install the 28 mm thick glass unit. The timber frame is considered to be restored, consolidated and milled for enlarging the profile and hosting the IGU. Since the IGU is a unique panel and not subdivided in more panels as the existing single glasses, the glass bars currently present on the sashes are removed, see Fig. 3.5.5.1. Also in scenario 5, similarly to scenario 4, all the activities of scenario 2 and 3 are included.

In Table 1 in Supplementary material the iteration frequency for all the activities to be undertaken in scenario 5 are reported and the considered components SL are given in Table 3.5.2. In total, 16 alternatives were modelled considering both SL and activities iteration frequency. The LC operating energy variation consequent to the implementation of the activities in scenario 5, is shown in Fig. 13 in Supplementary material.

The LC operating energy saving allowed by scenario 5 at the end of the considered building RL, ranges between 18.75% and 20.68%. It is worth noting that the maximum energy saving achievable by undertaking existing glass pane replacement with a double glazed IGU, is slightly lower than the maximum one allowed by the most simple alternative from scenario 4, namely adding a single glass pane to the historic windows. Indeed the most effective alternative from scenario 5 (sub-scenario 5.8.b) and the one of scenario 4.α (sub-scenario 4.α.7.b) allow respectively 20.68% and 20.90% life cycle operating energy reduction over 100 years. However, if considering the small difference in terms of operating energy saving (0.22%), the scenario 5 may reveal less environmental effective if accounting also the retrofitting embodied impacts. However, the assessment of the EERI embodied impacts are out of the scope of this study.

In scenario 5, the use of IGU with 35 years SL instead of 25, yields LC operating energy saving higher by up to 0.63% over 100 years. Although this extra operating energy saving is negligible, it not only confirms once again that more durable materials are likely to allow larger energy savings, but it also stresses again the need of assessing the retrofitting measures embodied impacts next to the operating energy saving when evaluating the environmental convenience of EERI.

4.6. Scenario 6 results: windows replacement

In the present case study, the total replacement of the historic fenestration with three different replacement windows allowed to obtain an initial energy consumption reduction from 182,120.45 to 138,540.04 kW h in case of aluminium frame, to 139,564.04 kW h in case of PVC frame and to 137,715.86 kW h in case of timber frame.

Although from the initial energy saving it resulted that the largest contribution was allowed by timber windows frame, in Section 4 it was observed that, if considering the fraction of performance decay, the timber windows perform non-conveniently due to the high fraction of energy saving loss (7.86%). This technical decay is given mainly by the deterioration of the paint layer. Indeed, it is supposed that the high initial thermal resistance of the timber frame deteriorates (at the end of the frame SL) until the value of the non-maintained windows (scenario 1). This is obviously a cautionary scenario.

It was observed that aluminium and PVC replacement windows, thanks to their low technical perishability, allow larger residual energy saving. However, if taking into account materials durability and interventions iteration frequency, the mentioned considerations are no longer viable.

In Table 1 in Supplementary material the iteration frequency for all the activities to be undertaken within scenario 6 (alternatives 6.A; 6.PVC and 6.T) are reported. The considered components SL are given in Table 3.5.2. In total, it were modelled 16 alternatives per replacement window frame material, 48 modelled alternatives in total.

The LC operating energy variation consequent to the implementation of the activities in scenario 6, is shown in Fig. 15 in Supplementary material for aluminium replacement windows, in Fig. 16 in Supplementary material for PVC replacement windows and in Fig. 17 in Supplementary material for timber replacement windows.

The life cycle operating energy saving allowed by scenario 6.A (aluminium) at the end of the considered building RL, ranges between 21.06% and 23.29%; for scenario 6.PVC (PVC) it ranges between 20.29% and 22.64% and for scenario 6.T (timber) it ranges between 20.02% and 23.26%. As a first, it should be observed that, the most effective results are allowed by aluminium and timber replacement windows and in a less extent by PVC.

Although the least effective aluminium replacement alternative allows to obtain up to 1.04% larger energy saving compared to the timber one (6.A.3.a versus 6.T.3.a), the most effective aluminium sub-scenario allows to obtain only 0.03% larger energy saving compared to the timber one (6.A.8.b versus 6.T.8.b). This makes the two scenarios in fact identical in terms of LC operating energy reduction potential. The best timber sub-scenario considers equal sealing profiles replacement frequency as the aluminium one and it additionally considers 5-years based timber frame maintenance. This means that, despite the large performance decay, as discussed in Section 4, if timber replacement

windows are properly maintained, they allow identical results as the aluminium replacement windows and even higher energy saving if compared to PVC replacement windows.

In scenario 6 alternatives it was observed that, the use of more durable materials (sealants and IGU with 20 and 35 years SL) allows to achieve up to 0.89% additional energy saving in comparison with the less durable ones (sealants and IGU with 10 and 25 years SL).

According to the obtained results, it can be concluded that windows replacement is not the most effective scenario "by definition". Indeed, with regard to the aluminium replacement windows, 10 alternatives out of 16 allow energy saving lower than the most effective alternative from scenario 4.γ. With regard to PVC replacement windows, only 1 alternative (6.PVC.8.b) performs better than scenario 4.γ; moreover, 5 alternatives out of 16 perform worse than the best alternative in scenario 4.α. and 3 alternatives perform worse than the best alternative of scenario 5; see Table 2 in Supplementary material.

With regard to timber replacement windows, it can be said that 4 alternatives out of 16, perform worse than the best alternative from scenario 4.α, 3 alternatives perform worse than the best alternative of scenario 5 and only 5 alternatives perform better than the best alternative from scenario 4.γ.

5. Conclusions

In this study, different fenestration improvement scenarios for a heritage building in Antwerp (Belgium) were investigated. The interventions, ranging between windows maintenance and windows replacement, were assessed by considering their effect on the building LC operating energy reduction within a time interval of 100 years.

The results highlighted that performing windows maintenance allows to contain life cycle operating energy by up to 3.56%. Larger energy savings (up to 5.93%) may be obtained if the maintenance is combining with windows drought proofing. According to these results it was evidenced, the validity of performing building maintenance in order to increase building energy efficiency as theoretically advised by the recent EN 16883 [75].

Nevertheless, given the low energy saving obtainable from maintenance, it should be evaluated if this intervention is still effective for reducing building LC environmental impacts when including also initial and recurrent materials embodied impacts. The latter will be object of further studies.

Next to maintenance and drought proofing, two other scenarios with low impact on the historic fenestration were modelled: the addition of a secondary glazing (both single and double glazed), and the replacement of the existing glass panes with an Insulating Glass Unit. Among these options, the addition of an internal double-glazed secondary glazing may allow to obtain the largest results (up to 22.45%) followed by the installation of a single-glazed secondary glazing (up to 20.90%) and the replacement of the existing single glass panes with an Insulating Glass Unit (20.68%). In all the scenarios it was observed that the use of more durable components allows to obtain more effective results.

Nevertheless, materials durability should be not meant solely as SL length of a given component (as too often interpreted), but most likely it should be considered as the relation between component performance and its SL length. If components allow for tiny energy saving, the elongation of their SL does not bring to remarkable additional energy life cycle energy saving (see scenario 3).

Finally, more destructive options, consisting in the historic windows replacement, were modelled. When considering the life cycle operating energy saving allowed by the alternatives: aluminium, PVC and timber replacement windows, it was observed that windows with large technical loss decay, such as timber windows, can allow competitive results if properly maintained.

According to the modelled options it resulted that aluminium and timber replacement windows allowed the largest life cycle operating energy reduction (respectively up to 23.39% and 23.26%), while PVC the smallest (up to 22.64%). However, this does not mean that aluminium and timber replacement windows allow always the most effective results. Indeed, according to the results, it is not possible to identify only one "most performing windows retrofitting option". This because the retrofitting measure effectiveness depends on the complex relation between materials durability (meaning the relation between energy saving fraction of a given component and its SL) and intervention iteration frequency. It was found indeed, that several alternatives within the replacement scenarios, were less effective than the simple addition of a single or double glazed secondary glazing or than the replacement of the existing glazing.

The obtained results suggest that, when discriminating among EERI, especially when implemented in historic and heritage buildings, it may be a good practice to explore several options without strongly relaying on measures traditionally considered effective. This approach would possibly reduce the ongoing frequent implementation of destructive EERI on historic and heritage buildings. This study will be followed up by an analysis of the environmental effectiveness of the presented measures by considering their initial and recurrent embodied impacts.

Acknowledgments

The research was financed by IWT – Instituut voor Innovatie door Wetenschap en Technologie, Belgium (131439).

Appendix A. Supplementary material

Supplementary data associated with this article can be found in the online version at http://dx.doi.org/10.1016/j.jobe.2018.02.006.

References

[1] A. Gustavsen, B.P. Jelle, State-of-the-Art Highly Insulating Window Frames – Research and Market Review, Oslo, 2007.
[2] N. Ginks, B. Painter, Energy retrofit interventions in historic buildings: exploring guidance and attitudes of conservation professionals to slim double glazing in the UK, Energy Build. 149 (2017) 391–399.
[3] V. Pracchi, N. Rat, A. Verzeroli, Historic windows: conservation or replacement what's the most sustainable intervention? Legislative situation, case studies and current research, in: Proceedings of the International Conference Energy Efficiency in Historic Buildings, no. 9, 2014.
[4] T. Nypan, Effects of European Union Legislation on the Built Cultural Heritage, Oslo, 2009.
[5] B. van Bommel, D. Schulz, Venster onder vuur, inleiding bij WTA studiedag van 23 maat 2012, in: Historische vensters: typologie, duurzaamheid, antiek glas, ramen, kozijnen, 2012, pp. 1–13.
[6] Glass For Europe, The Revision of the Energy Efficiency Action Plan, Brussels, 2010.
[7] D. Pickles, M. Ian, Wood Chris, N. Molyneux, E. Makri, Traditional Windows, Their Care, Repair and Upgrading, 1st ed., Historic England, UK, 2015.
[8] S. Fossdal, Windows in Existing Buildings – Maintenance, Upgrading Or Replacement? Oslo, 1996.
[9] A. Thomas, C.C. Menassa, V.R. Kamat, A framework to understand effect of building systems deterioration on life cycle energy, Procedia Eng. 118 (2015) 507–514.
[10] A. Thomas, S.M. Asce, C.C. Menassa, D. Ph, A.M. Asce, V.R. Kamat, D. Ph, A.M. Asce, System Dynamics Framework to Study the Effect of Material Performance on a Building's Lifecycle Energy Requirements, vol. 30, no. 6, 2016, pp. 1–15.
[11] C. Rudbeck, Methods for Designing Building Envelope Components Prepared for Repair and Maintenance, Technical University of Danimark, Kongens Lyngby (Denmark), 1999.
[12] European Union, Directive 2002/91/EC of the European Parliament and of European Council of 16 December 2002 on the Energy Performance of Buildings, 2002, pp. 65–71.
[13] European Union, Directive 2010/31/EU of the European Parliament and of the Cauncil of Europe of 19 May 2010 on the Energy Performance of Buildings (recast), 2010, pp. 13–35.
[14] J.O. Lewis, S.N. Hógáin, A. Borghi, Building Energy Efficiency in European Cities – URBACT II Capitalisation, Urbact Ii, 2013, pp. 1–52.
[15] BPIE: Building Performance Institute of Europe, Europe's Buildings under the Microscope, 2011.
[16] Building Performance Insitute of Europe, A Guide to Developing Strategies for Building Energy Renovation, Brussels, 2013.
[17] European Union, Directive 2012/27/EU of the European Parliament and Council of Europe of 25 October 2012 on Energy Efficiency, Amending Directives 2009/125/EC and 2010/30/EU and Repealing Directives 2004/8/EC and 2006/32/EC, Brussel

(Belgium), no. October 2012, pp. 1–56.
[18] V. Farinelli, L. Gabrielli, La stima di un bene storico-architettonico, le variabili significative nel caso delle Ville Venete, Recuper. Conserv. 126 (45) (2015) 2–14.
[19] B. James, A. Shapiro, S. Flanders, Testing the Energy Performance of Wood Windows in Cold Climates A Report to the State of Vermont Division for Historic Preservation Agency of Commerce and Community Development, Vermont (USA), 1996.
[20] Federal Commission for Historic Buildings, Windows of Historic Buildings, Fundamental Aspects, Switzerland, 2003.
[21] R.S. Adhikari, E. Lucchi, V. Pracchi, Historical Buildings: Energy Performance and Enhancement, 2013, pp. 1312–1320.
[22] B. Daniotti, Durabilità e Manutenzione edilizia (Durability and Building Maintenance), UTET scien, Milanofiori Assago (Milan), 2012.
[23] P.G. Cesarotto, M. De Carli, A measuring campaign of thermal conductance in situ and possible impacts on net energy demand in buildings, Energy Build. 59 (2013) 29–36.
[24] A. Abdou, I. Budaiwi, The variation of thermal conductivity of fibrous insulation materials under different levels of moisture content, Constr. Build. Mater. 43 (2013) 533–544.
[25] I. Budaiwi, A. Abdou, The impact of thermal conductivity change of moist fibrous insulation on energy performance of buildings under hot–humid conditions, Energy Build. 60 (2013) 388–399.
[26] E.V.A. Litavcová, M. Pavluš, J.Á.N. Seman, T. Bačinský, Moisture presence in building materials: deterioration of building energy properties, in: Proceedings of the 5th Central European Conference in Regional Science – CERS, 2014, pp. 500–508.
[27] G. Litti, S. Khoshdel, A. Audenaert, J. Braet, Hygrothermal performance evaluation of traditional brick masonry in historic buildings, Energy Build. 105 (2015) 393–411.
[28] L. Ortega Madrigal, B. Serrano Lanzarote, J.M. Fran Bretones, Proposed method of estimating the service life of building envelopes, Rev. Constr. 14 (1) (2015) 60–68.
[29] A. Silva, J. de Brito, P.L. Gaspar, Service life and durability of assemblies, in: Methodologies for Service Life Prediction a Focus on Facade Claddings, Springer International Publishing, 2016, pp. 13–61.
[30] R. Hendrickx, H. De Clercq, F. Decock, F. Descamps, Hygrothermal Analysis of the Façades of the Former Veterinary School in Anderlecht (Belgium) for the Risk Assessment of Internal Thermal Insulation, 2013, pp. 1092–1098.
[31] D. Browne, The SPAB Hygrothermal Modelling: Interim Report, no. October, 2012.
[32] F. Ochs, W. Heidemman, H. Müller-Steinhagen, Effective thermal conductivity of the insulation of high temperature underground thermal stores during operation, Ecostock 2006 (2006) 1–7.
[33] M. Jerman, R. Černý, Effect of moisture content on heat and moisture transport and storage properties of thermal insulation materials, Energy Build. 53 (2012) 39–46.
[34] A. Silva, J. de Brito, P.L. Gaspar, Comparative analysis of service life prediction methods, in: Methodologies for Service Life Prediction a Focus on Facade Claddings, Springer International Publishing, 2016, pp. 325–408.
[35] F. Shirley, F. Gamble, J. Galvin, A Comparative Study of the Cumulative Energy Use of Historical Versus Contemporary Windows, 2010.
[36] S.K. Asphaug, B.P. Jelle, L. Gullbrekken, S. Uvsløkk, Accelerated ageing and durability of double-glazed sealed insulating window panes and impact on heating demand in buildings, Energy Build. 116 (2016) 395–402.
[37] G. Litti, A. Audenaert, J. Braet, L. Lauriks, Energy environmental monitoring in historical buildings; a simplified methodology for modeling realistic retrofitting scenarios. The case study of Schoonselhof Kasteel in Antwerp (Belgium), in: Built Heritage Monitoring Conservation Management, 2013, pp. 1075–1083.
[39] C. Verheyen, Van scon-sele tot begraafplaats, Bouwhistorisch en bouwfysisch onderzoek van het kasteel en de neerhoeve van het Schoonselhof Wilrijk, Hogeschool Antwerpen, 2006.
[40] J. Bertran, Houten schrijnwerk, erfgoed en comfort verenigem, Directie M. Brussels, 2008.
[41] CEN European Commitee for Standardization, NBN EN 13829 Thermal Performance of Buildings- Determination of Air Permeability of Buildings-Fan Pressurization Method (ISO 9972:1996, modified), 2001.
[42] M. Sherman, D. Dickerhoff, Air-Tightness of US dwellings, Berkeley, 1998.
[43] M.H. Sherman, Estimation of infiltration from leakage and climate indicators, Energy Build. 10 (1) (1987) 81–86.
[44] M.R. Basset, A Practical Study of Retrofit Airtightening Old Houses for Energy Efficiency, December 1996.
[45] F.R. d'Ambrosio Alfano, M. Dell'Isola, G. Ficco, B.I. Palella, G. Riccio, Experimental air-tightness analysis in mediterranean buildings after windows retrofit, Sustainability 8 (10) (2016) 1–9.
[46] E. Finlayso, R. Mitchell, D. Arasteh, THERM 2.0: For Analyzing Two-Dimensional Heat Transfer Through Buildings Products, California, no. June, 1998.
[47] IES, ApacheSim Calculation Methods, UK, 2012.
[48] NBN EN ISO, EN ISO 6946 Building Components and Building Elements – Thermal Resistance and Thermal Transmittance- Calculation Method (ISO 6946:2007), 2008.
[49] CIBSE, Environmental Design, Guide A, 7th ed., Page Bros, London, 2006.
[50] M.F. Mecklenburg, Determining the Acceptable Ranges of Relative Humidity and Temperature in Museums and Galleries, Part 1, 2007.
[51] J. Beetsma, A. Hofland, Life cycle analysis of alkyd emulsion based paint, Surf. Coat. Int. 10 (10) (1998) 491–494.
[52] J. Schmid, Seal Analysis in Use for Door and Window Systems' (Dichtungsanalyse im Einsatz bei Fenster- und Türsystemen), 2012.
[53] P.J. Nigrey, Prediction of Packaging Seal Life Using Thermoanalytical Techniques, 1997, p. 10.
[54] BCIS, Life Expectancy of Building Components, Surveyors' Experiences of Buildings in Use, A Practical Guide, Second ed., 2006.
[55] A. Tenants Swiss, Building Components Life Expectancy Tables, 2016.
[56] The Specifiers' Guide to Timber Windows, 2015.
[57] S. Garvin, The Durability of Double-Glazing Units, 2001, pp. 107–118.
[58] J. Douglas, Building Adaptation, 2nd ed., 33 Elsevier Ltd, UK, 2006.
[59] G. Totaro, Sui processi di manutenzione del costruito tutelato, convenienze economiche, sviluppi occupazionali ed altre esternalità positive, Politecnico di Milano, 2015.
[60] J. van der Kooi, Moisture Movements in Timber Window Frames, Delft, 1976, pp. 1–7.
[61] English Heritage, Energy Efficiency in Historic Buildings: Draught-Proofing Windows and Doors, 2010, pp. 1–16.
[62] E. Lucchi, V. Pracchi, Efficienza energetica e patrimonio costruito, Plitecnica, 2013.
[63] N. Smith, N. Isaacs, J. Burgess, I. Cox-Smith, Thermal performance of secondary glazing as a retrofit alternative for single-glazed windows, Energy Build. 54 (2012) 47–51.
[64] N. Smith, N. Isaacs, A cost benefit analysis of secondary glazing as a retrofit alternative for New Zealand households, Built Hum. Environ. Rev. 2 (1) (2009) 69–80.
[65] M. Coillot, E. Mankibi, R. Cantin, Heating, ventilating and cooling impacts of double windows on historic buildings in Mediterranean area, Energy Procedia 133 (2017) 28–41.
[66] J. Bertrand, B. Vander Brugghem, C. Rouffin, C. Segers, Houten schrijnwerk; Erfgoed en Comfort verenigen, Directie Monumenten en Landschappen van het Brussel Hoofdstedelijk Geweest, Brussels, 2008.
[67] CEN European Commitee for Standardization, EN 673:2011 Glass in Building – Determination of Thermal Transmittance (U value) – Calculation Method, Belgium, 2011.
[68] H.S.L.C. Hens, Building Physics Heat, Air and Moisture Fundamentals and Engineering Methods with Examples and Exercises, 2nd edition, Ernst & Sohn, Berlin, 2012.
[69] A. Olsson-Jonsson, Energy efficient windows for how long? in: Proceedings of the 7th Symposium on Building Physicsin the Nordic Countries, 2005, pp. 13–15.
[70] CEN European Commitee for Standardization, EN 1279:2002 Glass in Building – Insulating Glass Units- Part 3: Long Term Test Method and Requirements for Gas Leakage Rate and for Gas Concentration Tolerances, vol. 3, 2002.
[71] D. Arasteh, S. Selkowitz, J. Wolfe, The design and testing of a highly insulating glazing system for use with conventional window systems, J. Sol. Energy Eng. 3 (1989) 1–24.
[72] A. Troi, Z. Bastian (Eds.), Energy Efficiency Solutions for Historic Buildings, A Handbook, Birkhauser Verlag GmbH, Basel, 2015.
[73] M. Hershfield, Maintenance, Repair and Replacement Effects for Building Envelope Materials, Ottawa, 2002.
[74] K.M. Switala-Elmhurst, P.D. Candidate, L. Ap, Life cycle assessment of residential windows: saving energy with window restoration, in: Proceedings of the 50th ASC Annual International Conference, 2014.
[75] CEN European Commitee for Standardization, EN 16883 Conservation of Cultural Heritage — Guidelines for Improving the Energy Performance of Historic Buildings, no. 0, 2017.